On the Confluence of Data-Driven Techniques and Laser-Plasma Acceleration

Andreas Döpp[1,2,3], Faran Irshad[1], Sunny Howard[1,3], Jannik Esslinger[1], Nils Weisse[1], Christoph Eberle[1], Jinpu Lin[1], Robin Wang[3], Peter Norreys[3], Stefan Karsch[1,2]

[1] *Centre for Advanced Laser Applications, Faculty of Physics, LMU Munich*

[2] *Max Planck Institute for Quantum Optics (MPQ)*

[3] *Faculty of Physics, Oxford University*

On the Confluence of

Data-Driven Techniques and Laser-Plasma Acceleration


Physics
Data*
* Here I use „data-driven techniques" as an umbrella term that encompasses everything from traditional methods to modern AI.

Talk outline

… maintaining data ↔ water analogies

Phase I

Collect data

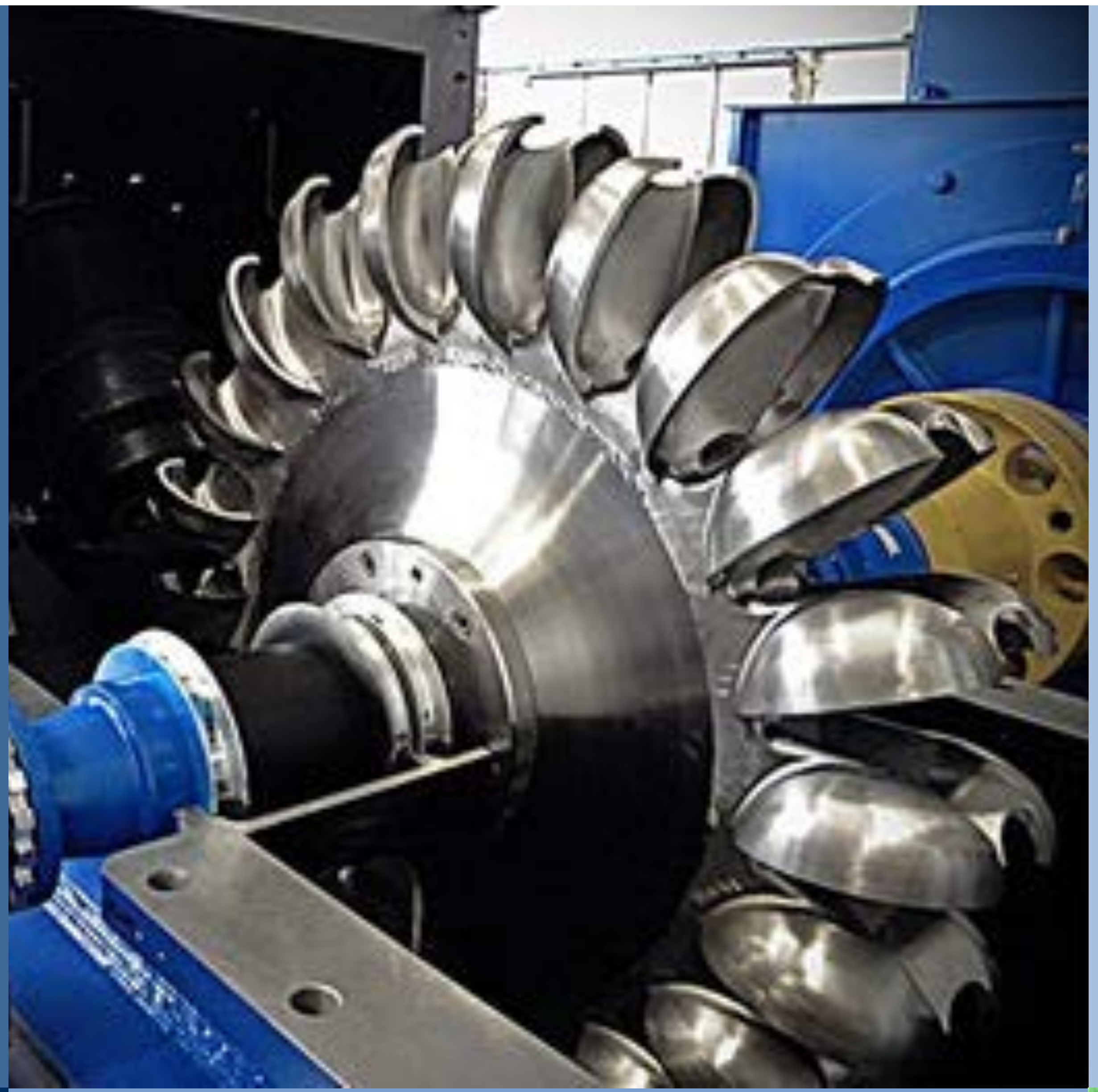

Phase III

Custom-made solutions
for your application

Phase II

Let the data work using

off-the-shelf methods

Phase I Data collection and control systems

From manual labor …

- Inside of vacuum chambers motorized, but gas regulation etc. manually
- Use camera manufacturer's software for data acquisition (some supported continuous sets, others have to be armed manually before each shot)
- Data logging: handwritten lab book
- Control system: Mix between proprietary software and LabView

Phase I Data collection and control systems

… to fully automized

CrossMark

High Power Laser Science and Engineering, (2023), Vol. 11, e44, 7 pages.
doi:10.1017/hpl.2023.17

HIGH POWER LASER SCIENCE AND ENGINEERING

RESEARCH ARTICLE

Tango Controls and data pipeline for petawatt laser experiments

Nils Weiße, Leonard Doyle, Johannes Gebhard, Felix Balling, Florian Schweiger, Florian Haberstroh, Laura D. Geulig, Jinpu Lin, Faran Irshad, Jannik Esslinger, Sonja Gerlach, Max Gilljohann, Vignesh Vaidyanathan, Dennis Siebert, Andreas Münzer, Gregor Schilling, Jörg Schreiber, Peter G. Thirolf, Stefan Karsch, and Andreas Döpp

Ludwig-Maximilians-Universität München, Garching, Germany

(Received 1 December 2022; accepted 16 February 2023)

Abstract
The Centre for Advanced Laser Applications in Garching, Germany, is home to the ATLAS-3000 multi-petawatt laser, dedicated to research on laser particle acceleration and its applications. A control system based on Tango Controls is implemented for both the laser and four experimental areas. The device server approach features high modularity, which, in addition to the hardware control, enables a quick extension of the system and allows for automated data acquisition of the laser parameters and experimental data for each laser shot. In this paper we present an overview of our implementation of the control system, as well as our advances in terms of experimental operation, online supervision and data processing. We also give an outlook on advanced experimental supervision and online data evaluation – where the data can be processed in a pipeline – which is being developed on the basis of this infrastructure.

Keywords: data processing; high-power laser experiments; laser–plasma acceleration; online diagnostics

1. Introduction

Petawatt laser facilities[1] enable the study of a plethora of phenomena, ranging from fundamental physics[2,3] and over laser-driven radiation sources[4–8] to applications with high societal relevance, such as medical imaging[9,10] and fusion energy[11]. However, the wide range of applications also results in a high variability of experimental configurations, and frequently shifting experimental requirements demand continuous modifications to the used technical infrastructure. The integration of new devices, such as motors, cameras or special instruments, into an experimental setup can be a time-consuming task for experimental physicists. Reliable control and supervision of all implemented devices is the first step in conducting any successful experiment. Thus, having a highly dependable and customizable server infrastructure that enables data acquisition and control of the entire experiment can be of great benefit for daily experimental work. However, this server infrastructure should still be easy to maintain and to work with because it must be used by many different employees and collaborating scientists from other facilities with specific needs and varying levels of programming experience. If these requirements are met, the server infrastructure then allows for even more advanced steps, such as online diagnostics, that enable the automation of the experiment and the implementation of safety features. In addition, a common server infrastructure standardizes the acquired data and streamlines the evaluation process into a data pipeline. The ongoing development of the data pipeline is planned to further enable advanced evaluation and control methods enabled by machine learning[12].

In this paper we are going to review the implementation of a control system that satisfies the requirements outlined above at the Centre for Advanced Laser Applications (CALA), its petawatt laser and experimental chambers[13,14]. The paper is structured as follows. Section 2 outlines the experimental infrastructure at CALA and the need for a common server infrastructure. An overview of the implemented control system, Tango Controls[15], and its basic features in terms of supervision and experimental operation is given

Correspondence to: Nils Weiße, Ludwig-Maximilians-Universität München, Am Coulombwall 1, 85748 Garching, Germany. Email: nils.weisse@physik.uni-muenchen.de

https://doi.org/10.1017/hpl.2023.17 Published online by Cambridge University Press

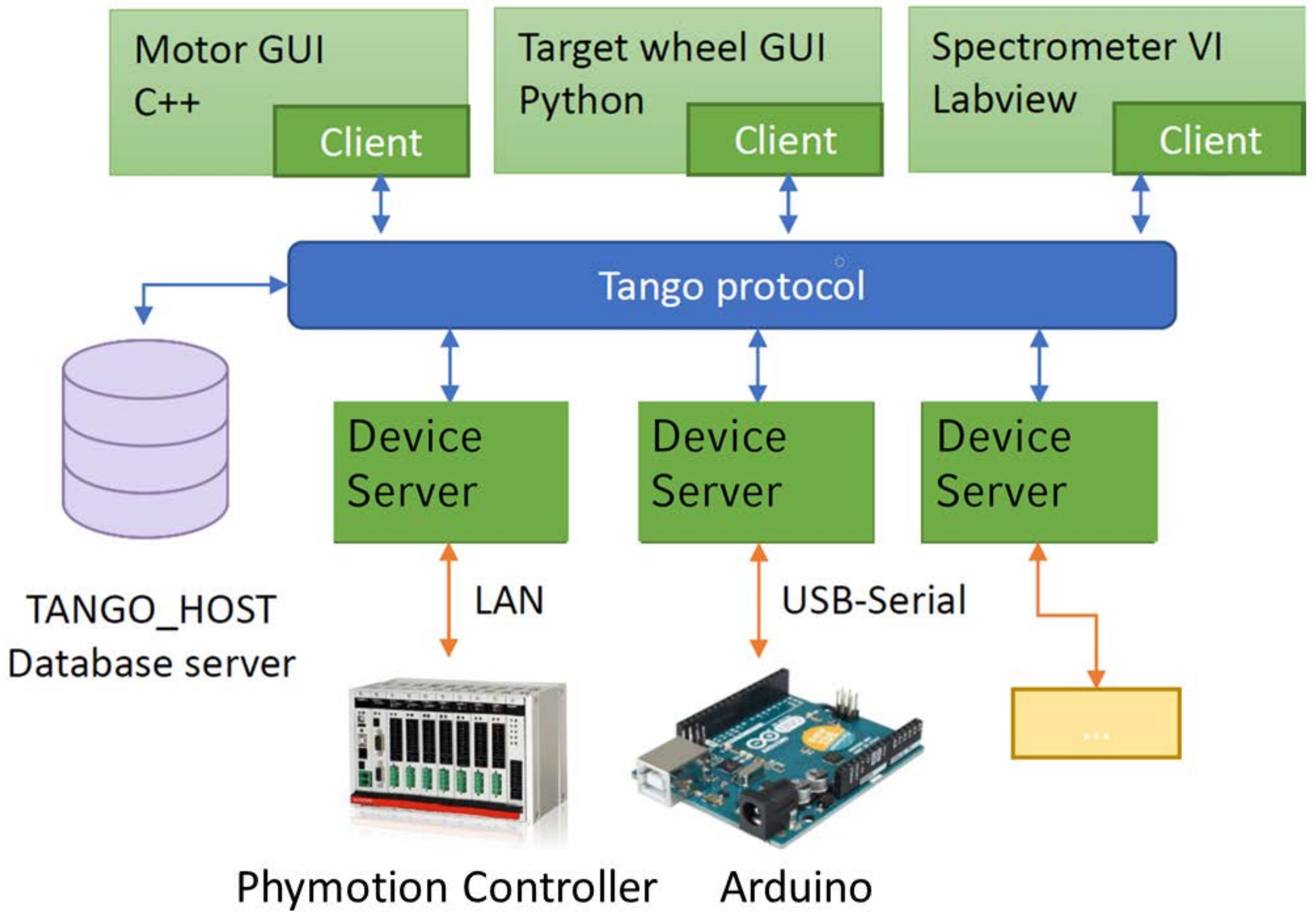

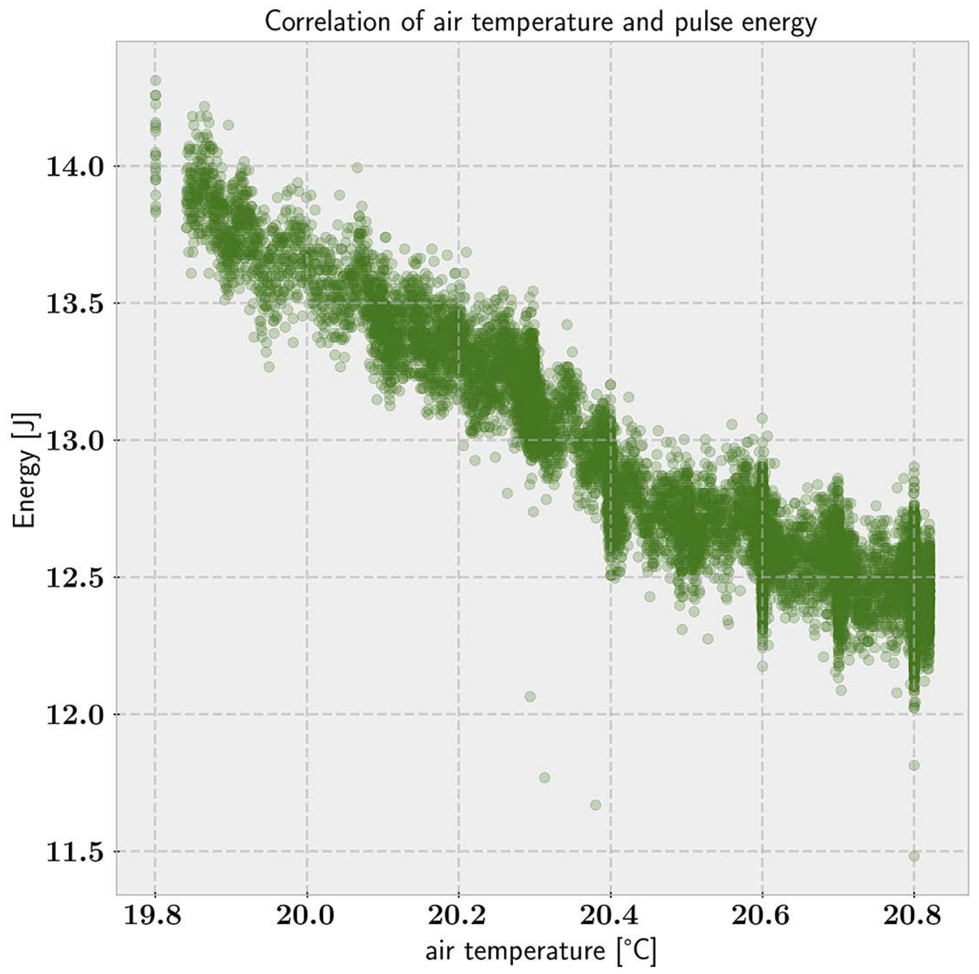

- Set up coherent acquisition and control system for both the laser and experiments based on TANGO controls
- On-going laboratory-wide effort, driven mostly by PhD students

Phase I Data collection and control systems

Review paper

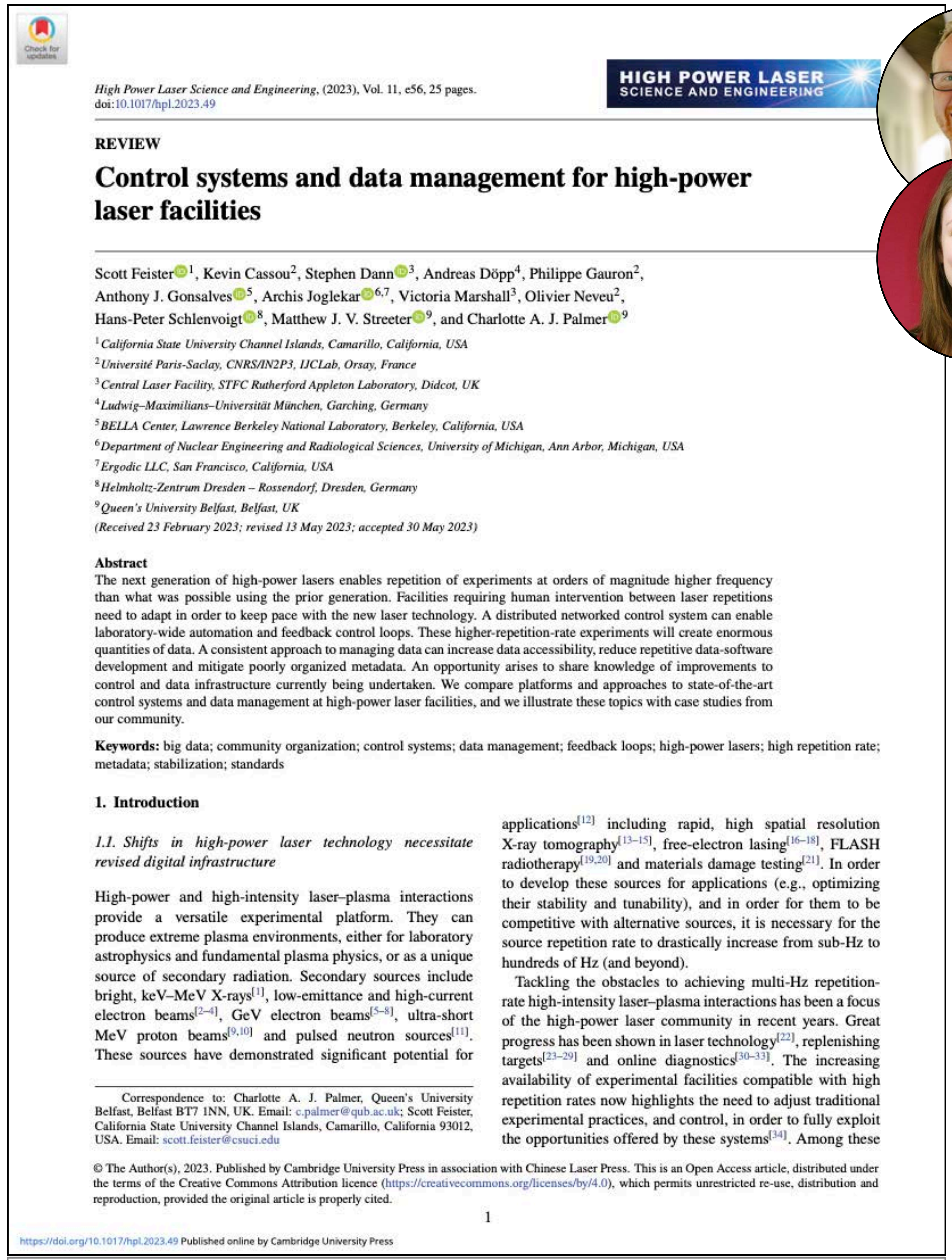
High Power Laser Science and Engineering, (2023), Vol. 11, e56, 25 pages.
doi:10.1017/hpl.2023.49

HIGH POWER LASER
SCIENCE AND ENGINEERING

REVIEW

Control systems and data management for high-power laser facilities

Scott Feister[1], Kevin Cassou[2], Stephen Dann[3], Andreas Döpp[4], Philippe Gauron[2], Anthony J. Gonsalves[5], Archis Joglekar[6,7], Victoria Marshall[3], Olivier Neveu[2], Hans-Peter Schlenvoigt[8], Matthew J. V. Streeter[9], and Charlotte A. J. Palmer[9]

[1] *California State University Channel Islands, Camarillo, California, USA*
[2] *Université Paris-Saclay, CNRS/IN2P3, IJCLab, Orsay, France*
[3] *Central Laser Facility, STFC Rutherford Appleton Laboratory, Didcot, UK*
[4] *Ludwig–Maximilians–Universität München, Garching, Germany*
[5] *BELLA Center, Lawrence Berkeley National Laboratory, Berkeley, California, USA*
[6] *Department of Nuclear Engineering and Radiological Sciences, University of Michigan, Ann Arbor, Michigan, USA*
[7] *Ergodic LLC, San Francisco, California, USA*
[8] *Helmholtz-Zentrum Dresden – Rossendorf, Dresden, Germany*
[9] *Queen's University Belfast, Belfast, UK*
(Received 23 February 2023; revised 13 May 2023; accepted 30 May 2023)

Abstract
The next generation of high-power lasers enables repetition of experiments at orders of magnitude higher frequency than what was possible using the prior generation. Facilities requiring human intervention between laser repetitions need to adapt in order to keep pace with the new laser technology. A distributed networked control system can enable laboratory-wide automation and feedback control loops. These higher-repetition-rate experiments will create enormous quantities of data. A consistent approach to managing data can increase data accessibility, reduce repetitive data-software development and mitigate poorly organized metadata. An opportunity arises to share knowledge of improvements to control and data infrastructure currently being undertaken. We compare platforms and approaches to state-of-the-art control systems and data management at high-power laser facilities, and we illustrate these topics with case studies from our community.

Keywords: big data; community organization; control systems; data management; feedback loops; high-power lasers; high repetition rate; metadata; stabilization; standards

1. Introduction

1.1. Shifts in high-power laser technology necessitate revised digital infrastructure

High-power and high-intensity laser–plasma interactions provide a versatile experimental platform. They can produce extreme plasma environments, either for laboratory astrophysics and fundamental plasma physics, or as a unique source of secondary radiation. Secondary sources include bright, keV–MeV X-rays[1], low-emittance and high-current electron beams[2–4], GeV electron beams[5–8], ultra-short MeV proton beams[9,10] and pulsed neutron sources[11]. These sources have demonstrated significant potential for applications[12] including rapid, high spatial resolution X-ray tomography[13–15], free-electron lasing[16–18], FLASH radiotherapy[19,20] and materials damage testing[21]. In order to develop these sources for applications (e.g., optimizing their stability and tunability), and in order for them to be competitive with alternative sources, it is necessary for the source repetition rate to drastically increase from sub-Hz to hundreds of Hz (and beyond).

Tackling the obstacles to achieving multi-Hz repetition-rate high-intensity laser–plasma interactions has been a focus of the high-power laser community in recent years. Great progress has been shown in laser technology[22], replenishing targets[23–29] and online diagnostics[30–33]. The increasing availability of experimental facilities compatible with high repetition rates now highlights the need to adjust traditional experimental practices, and control, in order to fully exploit the opportunities offered by these systems[34]. Among these

Correspondence to: Charlotte A. J. Palmer, Queen's University Belfast, Belfast BT7 1NN, UK. Email: c.palmer@qub.ac.uk; Scott Feister, California State University Channel Islands, Camarillo, California 93012, USA. Email: scott.feister@csuci.edu

1

https://doi.org/10.1017/hpl.2023.49 Published online by Cambridge University Press

- Overview about control systems written / coordinated by Scott Feister (California State U.) and Charlotte Palmer (QUB)
- Discusses different **design considerations**
- Case studies about
  - **LabView** at BELLA
  - **EPICS** at RAL
  - **Tango** at PALLAS

Phase II Apply established machine learning techniques

- What to do with my data?
- What are established machine learning techniques?
- Which method is suitable for my application?

Phase II Apply established machine learning techniques

Review paper

- What to do with my data?
- What are established machine learning techniques?
- Which method is suitable for my application?
- Extensive **review / tutorial paper** (30+ pages) on data-driven science and machine learning methods in laser-plasma physics

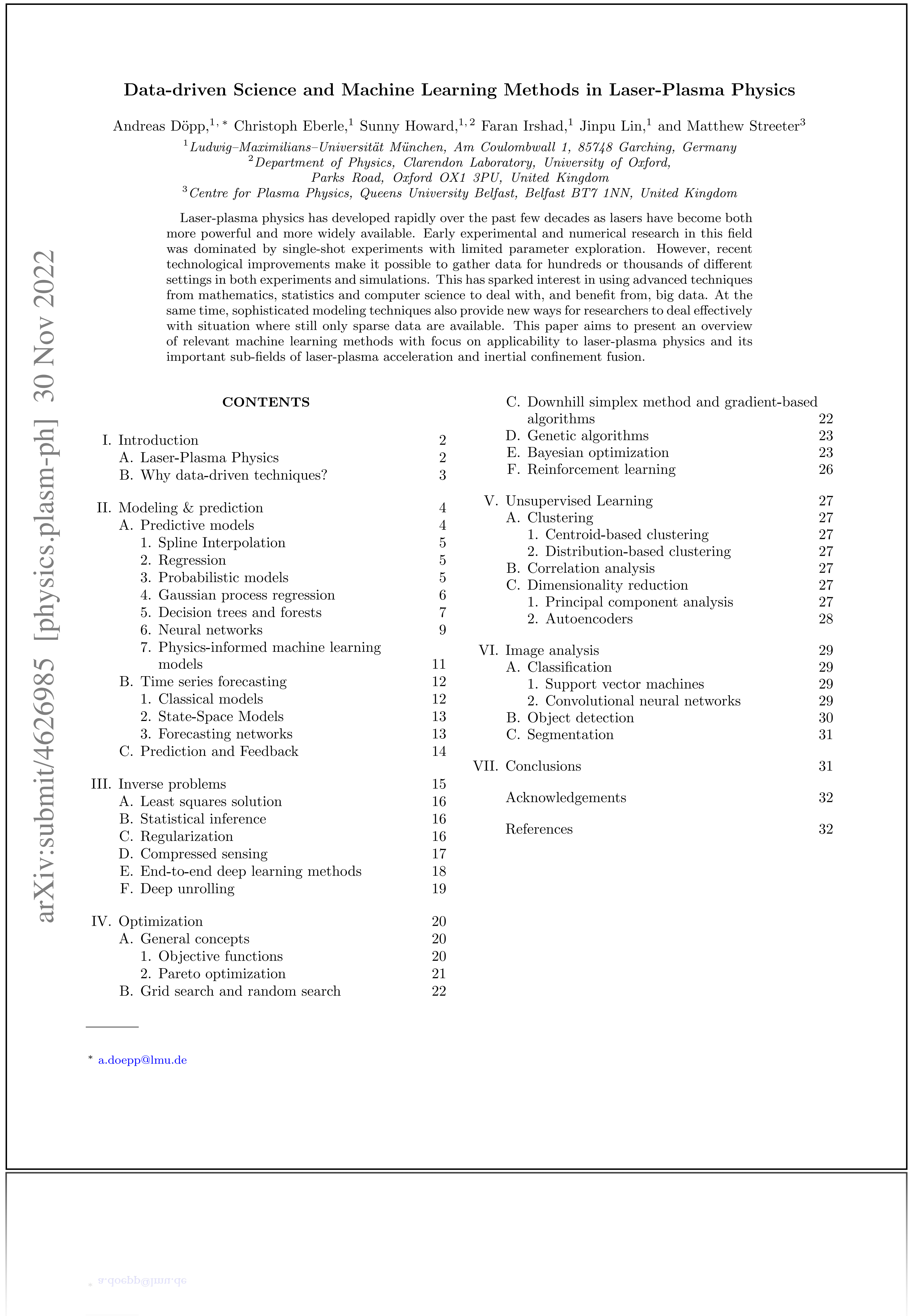

arXiv:submit/4626985 [physics.plasm-ph] 30 Nov 2022

Data-driven Science and Machine Learning Methods in Laser-Plasma Physics

Andreas Döpp,[1,*] Christoph Eberle,[1] Sunny Howard,[1,2] Faran Irshad,[1] Jinpu Lin,[1] and Matthew Streeter[3]

[1]*Ludwig–Maximilians–Universität München, Am Coulombwall 1, 85748 Garching, Germany*
[2]*Department of Physics, Clarendon Laboratory, University of Oxford, Parks Road, Oxford OX1 3PU, United Kingdom*
[3]*Centre for Plasma Physics, Queens University Belfast, Belfast BT7 1NN, United Kingdom*

Laser-plasma physics has developed rapidly over the past few decades as lasers have become both more powerful and more widely available. Early experimental and numerical research in this field was dominated by single-shot experiments with limited parameter exploration. However, recent technological improvements make it possible to gather data for hundreds or thousands of different settings in both experiments and simulations. This has sparked interest in using advanced techniques from mathematics, statistics and computer science to deal with, and benefit from, big data. At the same time, sophisticated modeling techniques also provide new ways for researchers to deal effectively with situation where still only sparse data are available. This paper aims to present an overview of relevant machine learning methods with focus on applicability to laser-plasma physics and its important sub-fields of laser-plasma acceleration and inertial confinement fusion.

CONTENTS

* a.doepp@lmu.de





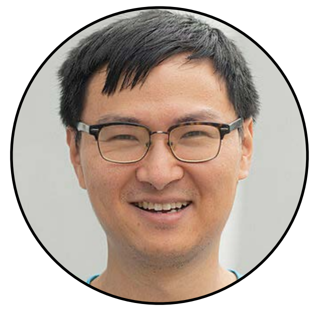


- A. Döpp et al. **Data-driven Science and Machine Learning Methods in Laser-Plasma Physics,** High Power Laser Science and Engineering **11** 55 (2023) | *arXiv:2212.00026* (2022)

Phase II Apply established machine learning techniques

Review paper

- What to do with my data?
- What are established machine learning techniques?
- Which method is suitable for my application?
- Extensive **review / tutorial paper** (30+ pages) on data-driven science and machine learning methods in laser-plasma physics

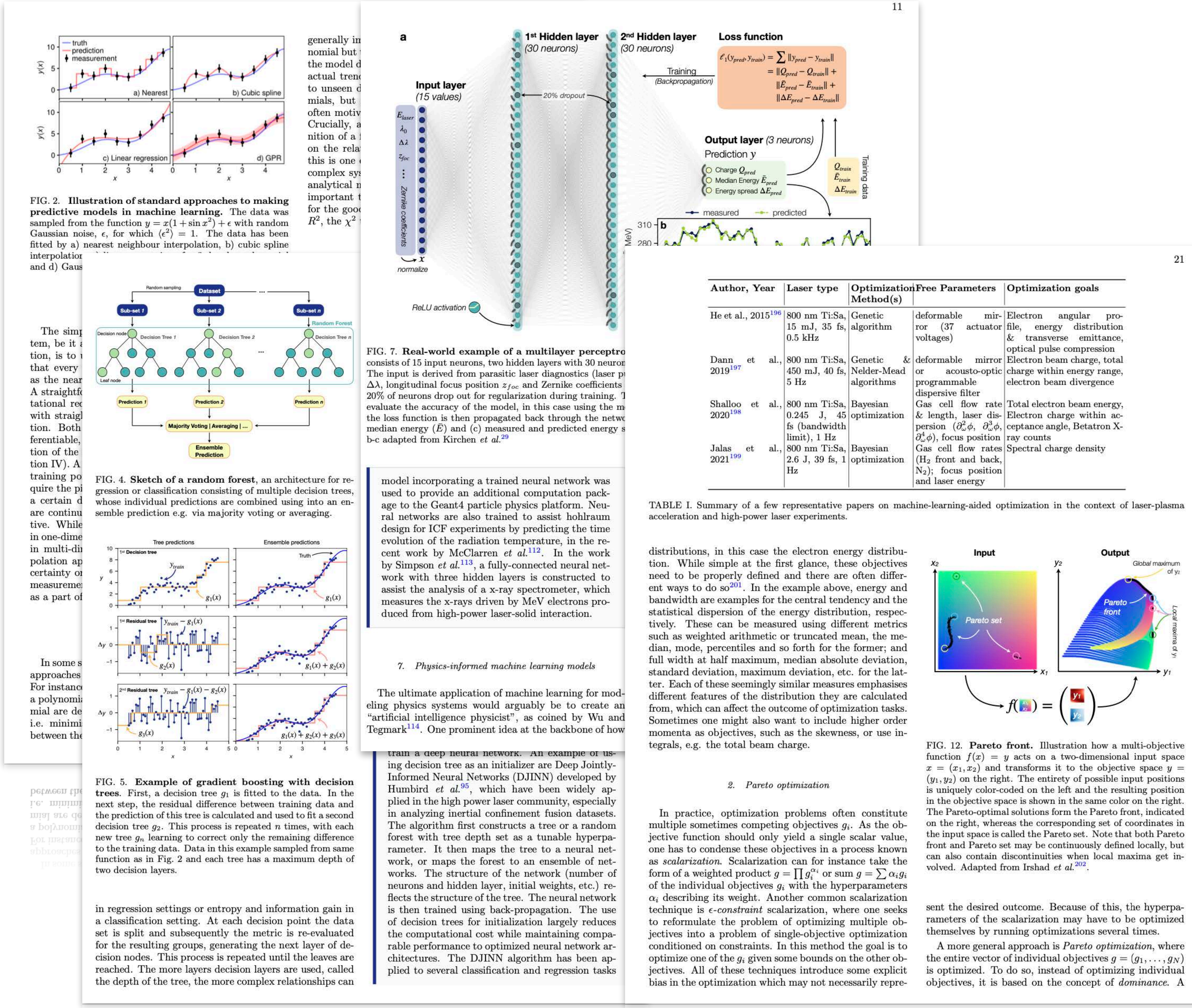

- A. Döpp et al. **Data-driven Science and Machine Learning Methods in Laser-Plasma Physics,** High Power Laser Science and Engineering **11** 55 (2023) | *arXiv:2212.00026* (2022)

Phase II Apply established machine learning techniques

Object detection using YOLOv5

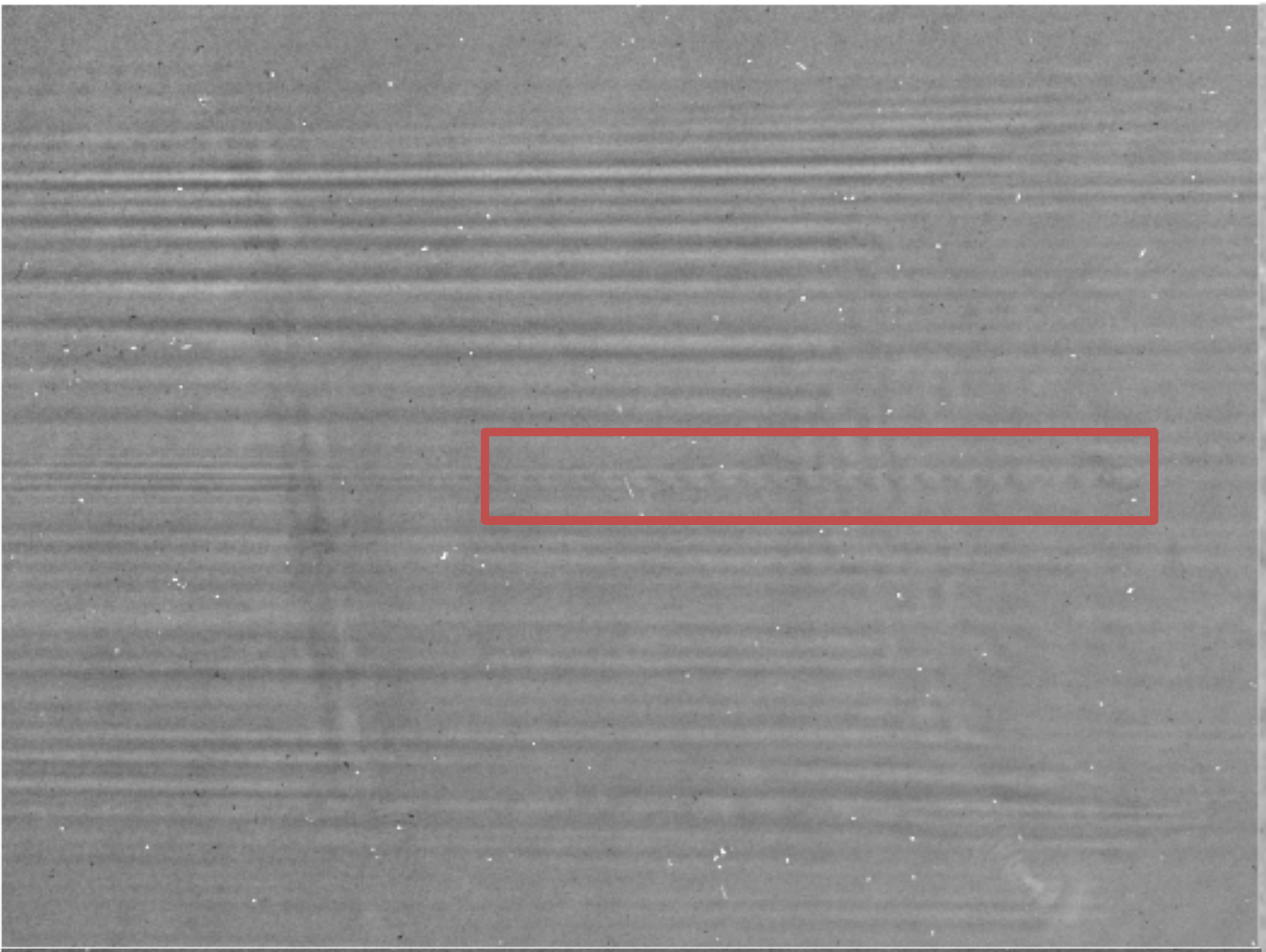

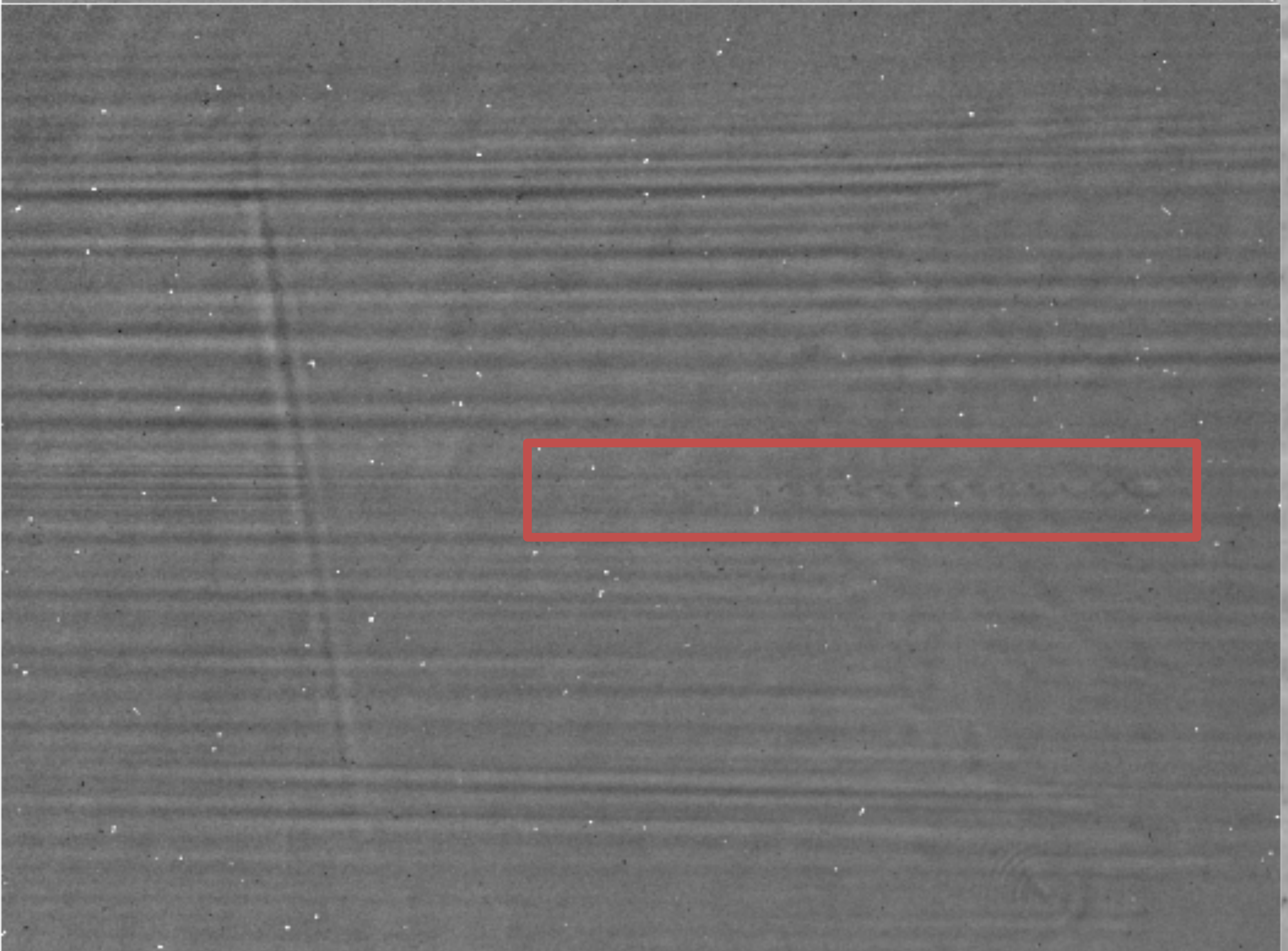

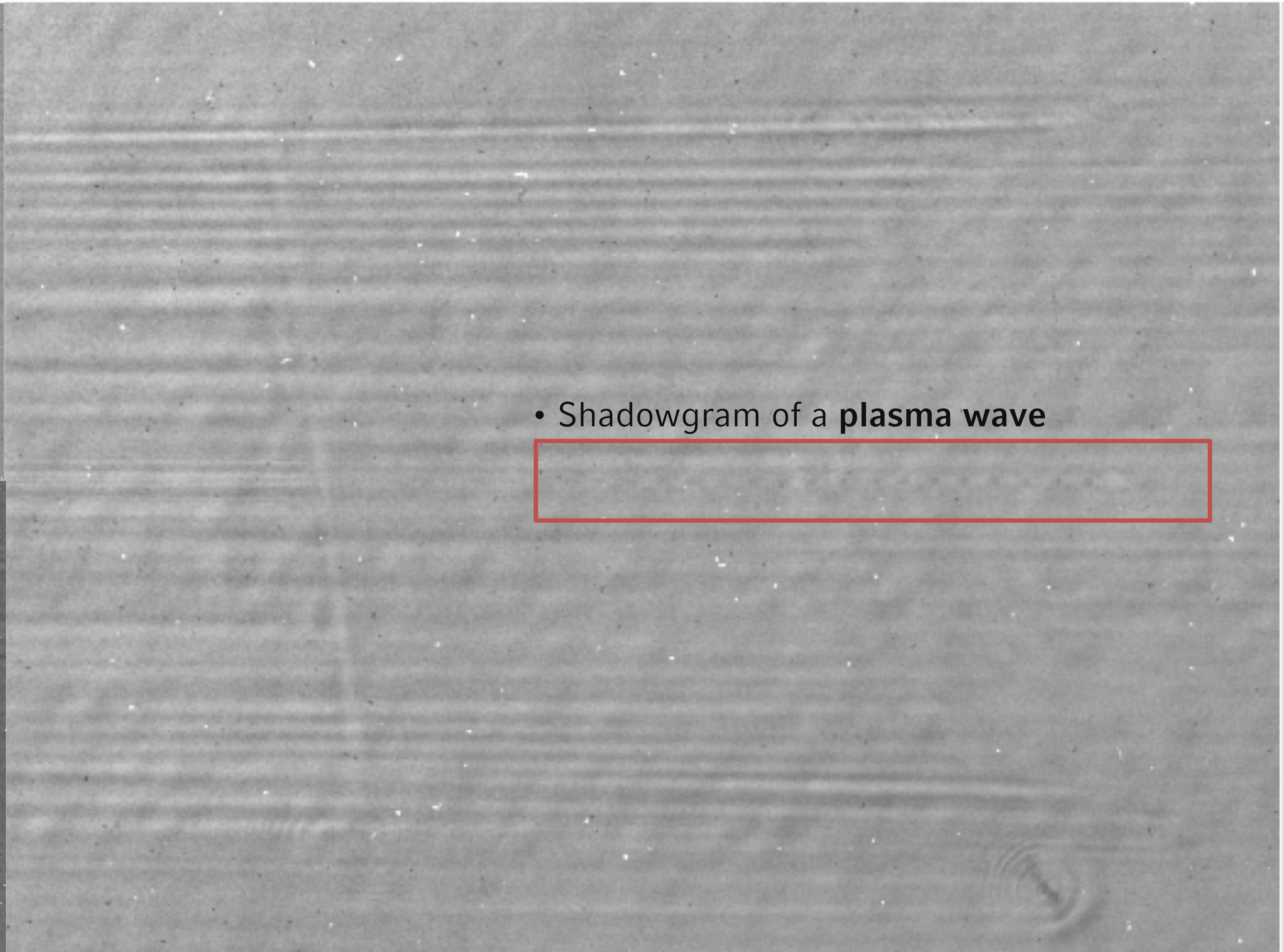

- Shadowgram of a **plasma wave**

Phase II Apply established machine learning techniques

Object detection using YOLOv5

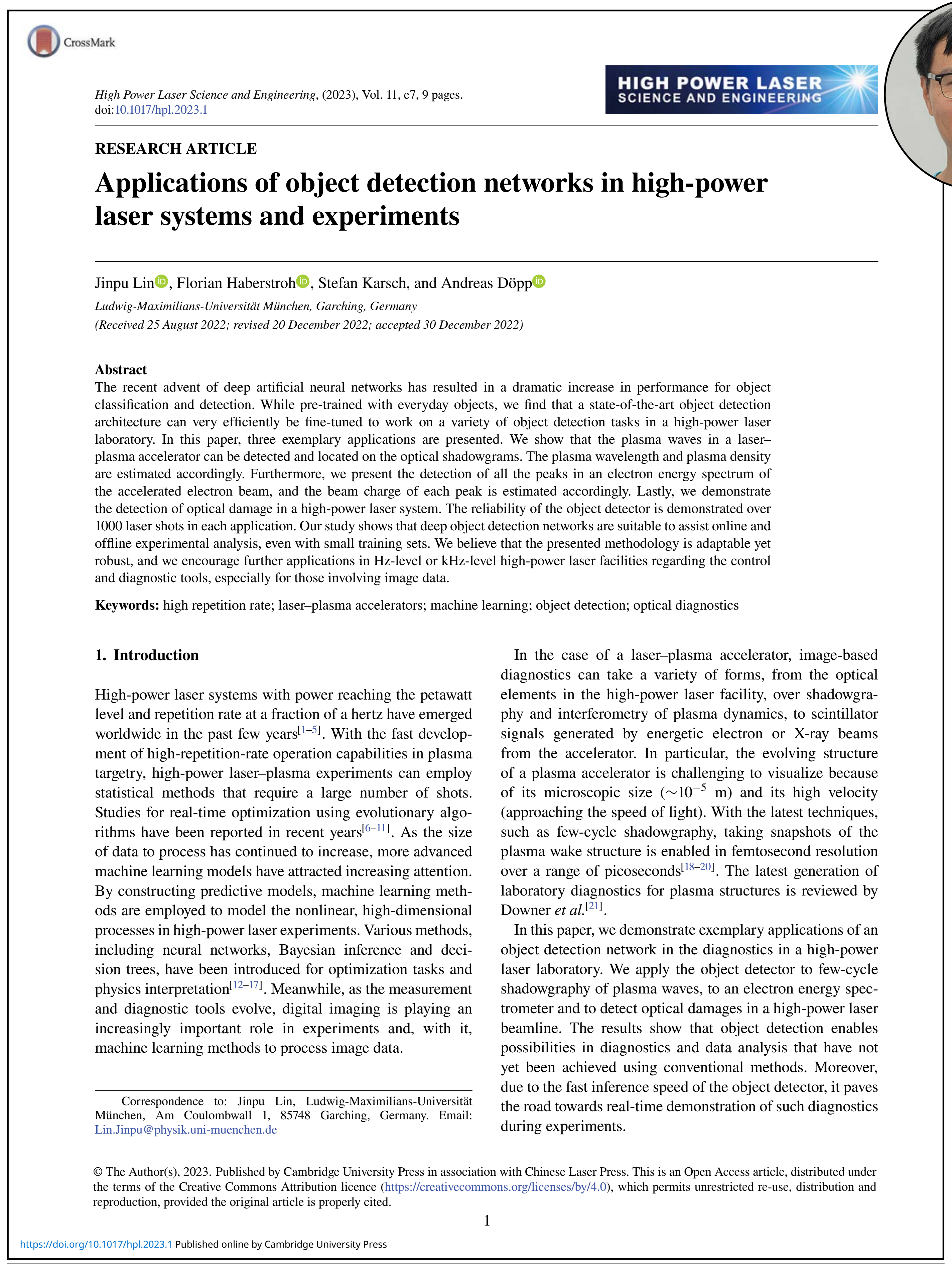
CrossMark

High Power Laser Science and Engineering, (2023), Vol. 11, e7, 9 pages.
doi:10.1017/hpl.2023.1

HIGH POWER LASER SCIENCE AND ENGINEERING

RESEARCH ARTICLE

Applications of object detection networks in high-power laser systems and experiments

Jinpu Lin, Florian Haberstroh, Stefan Karsch, and Andreas Döpp
Ludwig-Maximilians-Universität München, Garching, Germany
(Received 25 August 2022; revised 20 December 2022; accepted 30 December 2022)

Abstract
The recent advent of deep artificial neural networks has resulted in a dramatic increase in performance for object classification and detection. While pre-trained with everyday objects, we find that a state-of-the-art object detection architecture can very efficiently be fine-tuned to work on a variety of object detection tasks in a high-power laser laboratory. In this paper, three exemplary applications are presented. We show that the plasma waves in a laser–plasma accelerator can be detected and located on the optical shadowgrams. The plasma wavelength and plasma density are estimated accordingly. Furthermore, we present the detection of all the peaks in an electron energy spectrum of the accelerated electron beam, and the beam charge of each peak is estimated accordingly. Lastly, we demonstrate the detection of optical damage in a high-power laser system. The reliability of the object detector is demonstrated over 1000 laser shots in each application. Our study shows that deep object detection networks are suitable to assist online and offline experimental analysis, even with small training sets. We believe that the presented methodology is adaptable yet robust, and we encourage further applications in Hz-level or kHz-level high-power laser facilities regarding the control and diagnostic tools, especially for those involving image data.

Keywords: high repetition rate; laser–plasma accelerators; machine learning; object detection; optical diagnostics

1. Introduction

High-power laser systems with power reaching the petawatt level and repetition rate at a fraction of a hertz have emerged worldwide in the past few years[1–5]. With the fast development of high-repetition-rate operation capabilities in plasma targetry, high-power laser–plasma experiments can employ statistical methods that require a large number of shots. Studies for real-time optimization using evolutionary algorithms have been reported in recent years[6–11]. As the size of data to process has continued to increase, more advanced machine learning models have attracted increasing attention. By constructing predictive models, machine learning methods are employed to model the nonlinear, high-dimensional processes in high-power laser experiments. Various methods, including neural networks, Bayesian inference and decision trees, have been introduced for optimization tasks and physics interpretation[12–17]. Meanwhile, as the measurement and diagnostic tools evolve, digital imaging is playing an increasingly important role in experiments and, with it, machine learning methods to process image data.

In the case of a laser–plasma accelerator, image-based diagnostics can take a variety of forms, from the optical elements in the high-power laser facility, over shadowgraphy and interferometry of plasma dynamics, to scintillator signals generated by energetic electron or X-ray beams from the accelerator. In particular, the evolving structure of a plasma accelerator is challenging to visualize because of its microscopic size ($\sim 10^{-5}$ m) and its high velocity (approaching the speed of light). With the latest techniques, such as few-cycle shadowgraphy, taking snapshots of the plasma wake structure is enabled in femtosecond resolution over a range of picoseconds[18–20]. The latest generation of laboratory diagnostics for plasma structures is reviewed by Downer *et al.*[21].

In this paper, we demonstrate exemplary applications of an object detection network in the diagnostics in a high-power laser laboratory. We apply the object detector to few-cycle shadowgraphy of plasma waves, to an electron energy spectrometer and to detect optical damages in a high-power laser beamline. The results show that object detection enables possibilities in diagnostics and data analysis that have not yet been achieved using conventional methods. Moreover, due to the fast inference speed of the object detector, it paves the road towards real-time demonstration of such diagnostics during experiments.

Correspondence to: Jinpu Lin, Ludwig-Maximilians-Universität München, Am Coulombwall 1, 85748 Garching, Germany. Email: Lin.Jinpu@physik.uni-muenchen.de

https://doi.org/10.1017/hpl.2023.1 Published online by Cambridge University Press

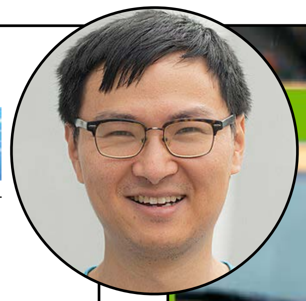

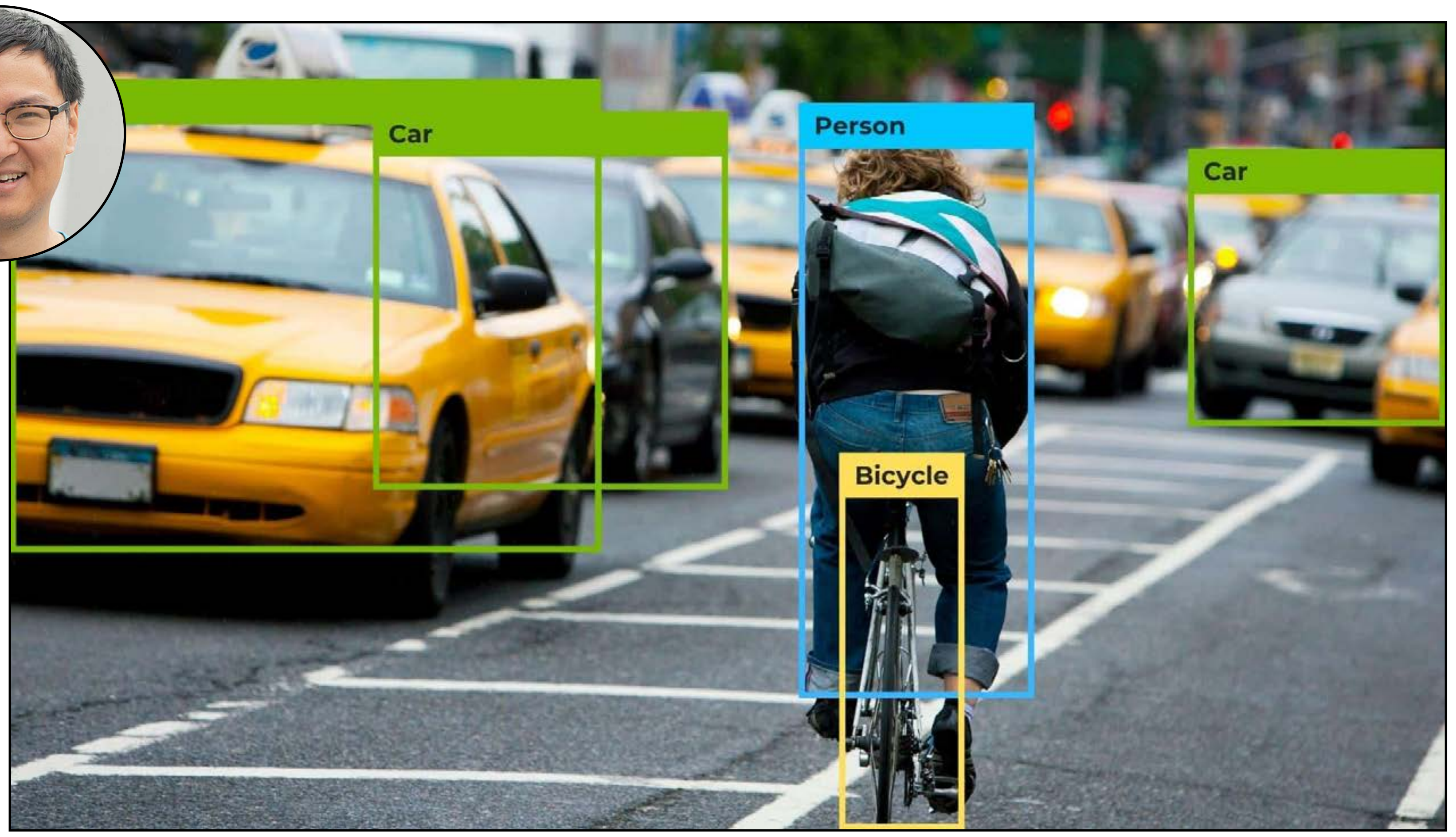

- Applied „off-the-shelf“ ML method
- You Only Look Once (YOLO) is an industry-standard object detection network

Phase II Apply established machine learning techniques

Object detection using YOLOv5

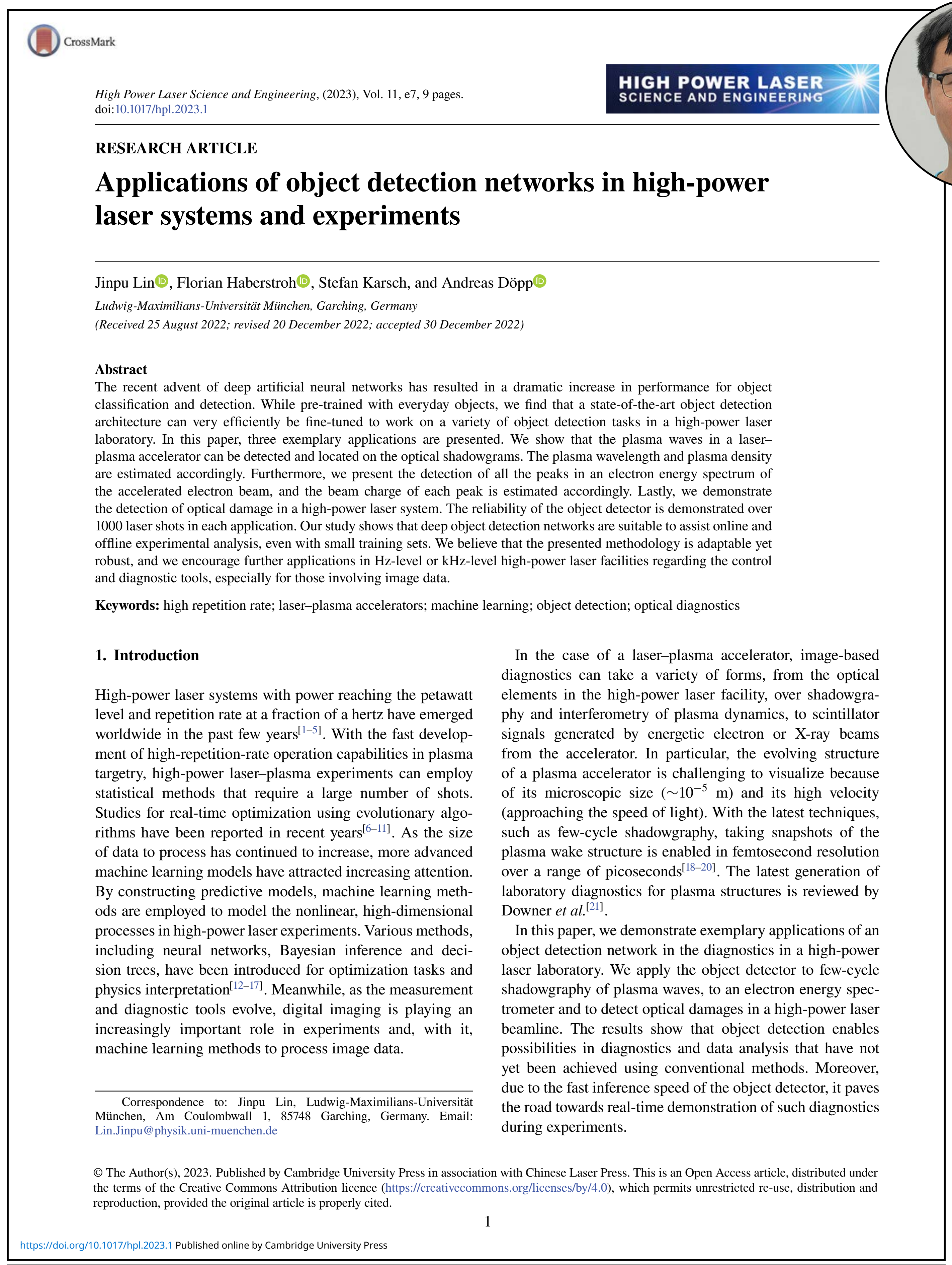

CrossMark

High Power Laser Science and Engineering, (2023), Vol. 11, e7, 9 pages.
doi:10.1017/hpl.2023.1

HIGH POWER LASER SCIENCE AND ENGINEERING

RESEARCH ARTICLE

Applications of object detection networks in high-power laser systems and experiments

Jinpu Lin, Florian Haberstroh, Stefan Karsch, and Andreas Döpp
Ludwig-Maximilians-Universität München, Garching, Germany
(Received 25 August 2022; revised 20 December 2022; accepted 30 December 2022)

Abstract
The recent advent of deep artificial neural networks has resulted in a dramatic increase in performance for object classification and detection. While pre-trained with everyday objects, we find that a state-of-the-art object detection architecture can very efficiently be fine-tuned to work on a variety of object detection tasks in a high-power laser laboratory. In this paper, three exemplary applications are presented. We show that the plasma waves in a laser–plasma accelerator can be detected and located on the optical shadowgrams. The plasma wavelength and plasma density are estimated accordingly. Furthermore, we present the detection of all the peaks in an electron energy spectrum of the accelerated electron beam, and the beam charge of each peak is estimated accordingly. Lastly, we demonstrate the detection of optical damage in a high-power laser system. The reliability of the object detector is demonstrated over 1000 laser shots in each application. Our study shows that deep object detection networks are suitable to assist online and offline experimental analysis, even with small training sets. We believe that the presented methodology is adaptable yet robust, and we encourage further applications in Hz-level or kHz-level high-power laser facilities regarding the control and diagnostic tools, especially for those involving image data.

Keywords: high repetition rate; laser–plasma accelerators; machine learning; object detection; optical diagnostics

1. Introduction

High-power laser systems with power reaching the petawatt level and repetition rate at a fraction of a hertz have emerged worldwide in the past few years[1–5]. With the fast development of high-repetition-rate operation capabilities in plasma targetry, high-power laser–plasma experiments can employ statistical methods that require a large number of shots. Studies for real-time optimization using evolutionary algorithms have been reported in recent years[6–11]. As the size of data to process has continued to increase, more advanced machine learning models have attracted increasing attention. By constructing predictive models, machine learning methods are employed to model the nonlinear, high-dimensional processes in high-power laser experiments. Various methods, including neural networks, Bayesian inference and decision trees, have been introduced for optimization tasks and physics interpretation[12–17]. Meanwhile, as the measurement and diagnostic tools evolve, digital imaging is playing an increasingly important role in experiments and, with it, machine learning methods to process image data.

Correspondence to: Jinpu Lin, Ludwig-Maximilians-Universität München, Am Coulombwall 1, 85748 Garching, Germany. Email: Lin.Jinpu@physik.uni-muenchen.de

In the case of a laser–plasma accelerator, image-based diagnostics can take a variety of forms, from the optical elements in the high-power laser facility, over shadowgraphy and interferometry of plasma dynamics, to scintillator signals generated by energetic electron or X-ray beams from the accelerator. In particular, the evolving structure of a plasma accelerator is challenging to visualize because of its microscopic size ($\sim 10^{-5}$ m) and its high velocity (approaching the speed of light). With the latest techniques, such as few-cycle shadowgraphy, taking snapshots of the plasma wake structure is enabled in femtosecond resolution over a range of picoseconds[18–20]. The latest generation of laboratory diagnostics for plasma structures is reviewed by Downer *et al.*[21].

In this paper, we demonstrate exemplary applications of an object detection network in the diagnostics in a high-power laser laboratory. We apply the object detector to few-cycle shadowgraphy of plasma waves, to an electron energy spectrometer and to detect optical damages in a high-power laser beamline. The results show that object detection enables possibilities in diagnostics and data analysis that have not yet been achieved using conventional methods. Moreover, due to the fast inference speed of the object detector, it paves the road towards real-time demonstration of such diagnostics during experiments.

https://doi.org/10.1017/hpl.2023.1 Published online by Cambridge University Press

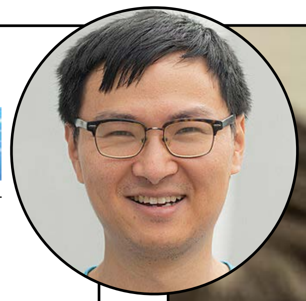

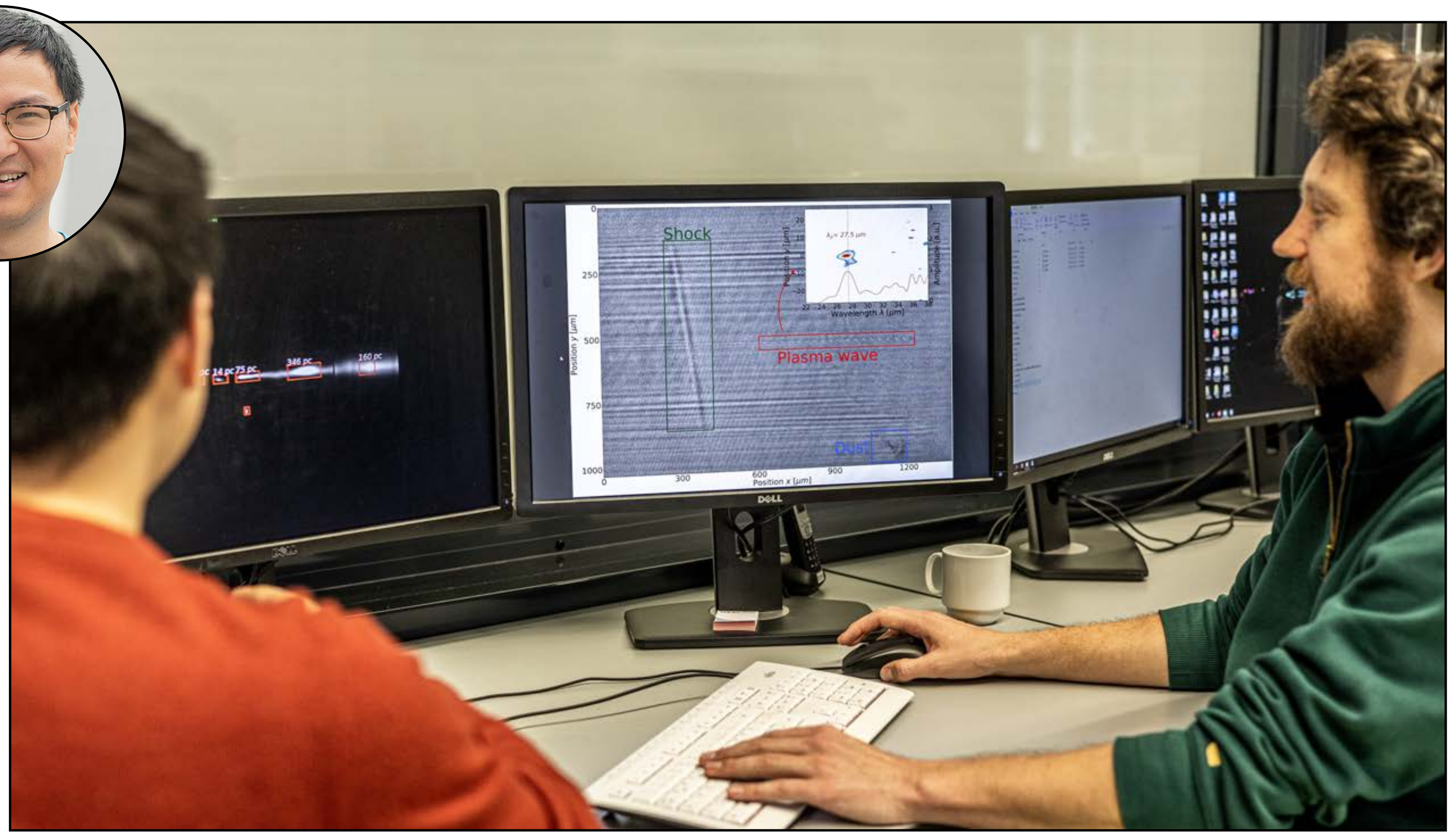

- Accurate predictions after fine-tuning with only 30-50 samples
- Works for plasma waves, laser damage, etc.

Labelled set size	Augmented set size	Time	Inference set of 50 accuracy	Inference set of 1000 accuracy
15	35	5 min	68%	52%
30	52	8 min	98%	85%
50	124	11 min	100%	97%

Phase II Apply established machine learning techniques

Object detection using YOLOv5

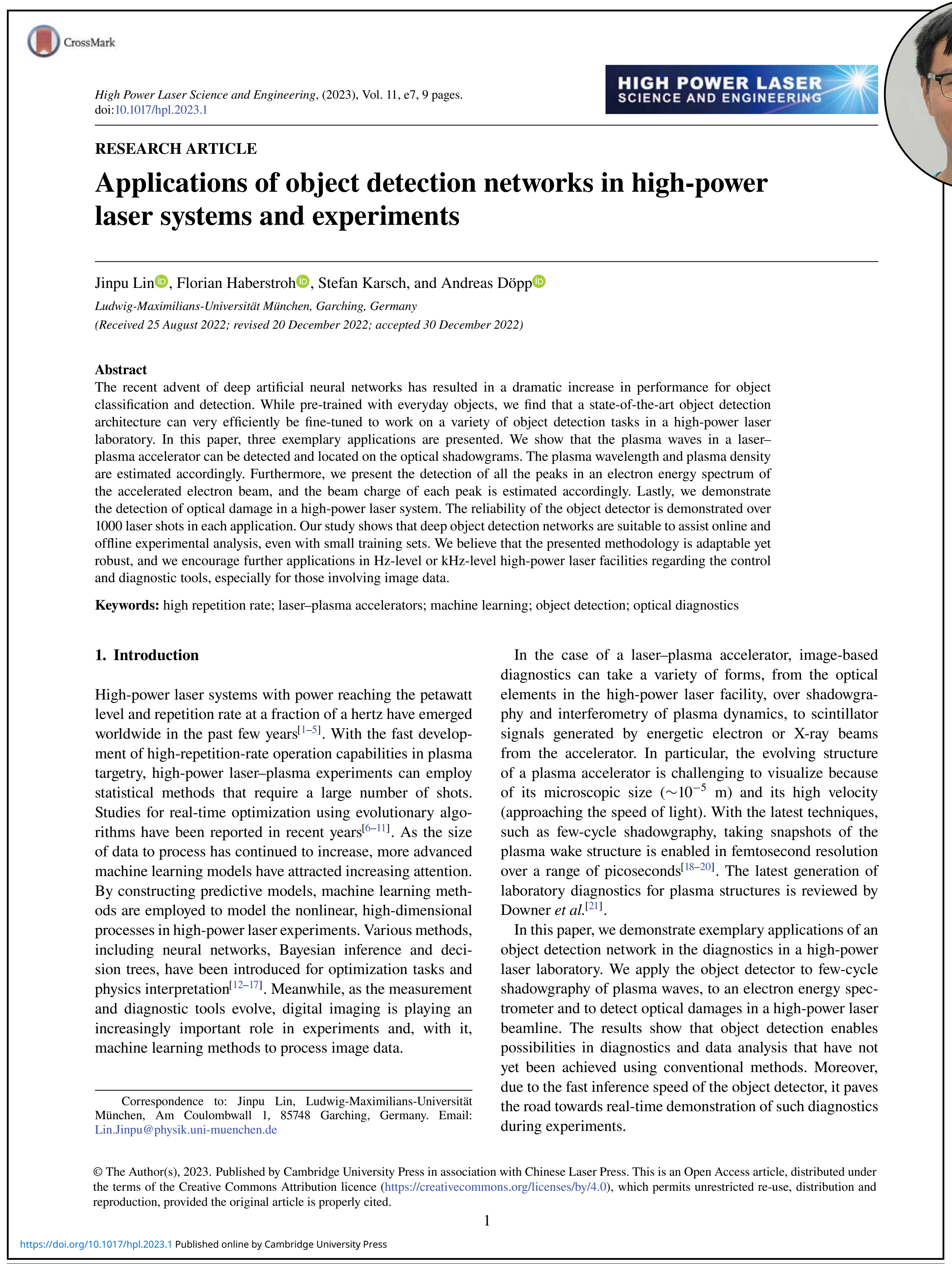

CrossMark

HIGH POWER LASER SCIENCE AND ENGINEERING

High Power Laser Science and Engineering, (2023), Vol. 11, e7, 9 pages.
doi:10.1017/hpl.2023.1

RESEARCH ARTICLE

Applications of object detection networks in high-power laser systems and experiments

Jinpu Lin, Florian Haberstroh, Stefan Karsch, and Andreas Döpp

Ludwig-Maximilians-Universität München, Garching, Germany

(Received 25 August 2022; revised 20 December 2022; accepted 30 December 2022)

Abstract

The recent advent of deep artificial neural networks has resulted in a dramatic increase in performance for object classification and detection. While pre-trained with everyday objects, we find that a state-of-the-art object detection architecture can very efficiently be fine-tuned to work on a variety of object detection tasks in a high-power laser laboratory. In this paper, three exemplary applications are presented. We show that the plasma waves in a laser–plasma accelerator can be detected and located on the optical shadowgrams. The plasma wavelength and plasma density are estimated accordingly. Furthermore, we present the detection of all the peaks in an electron energy spectrum of the accelerated electron beam, and the beam charge of each peak is estimated accordingly. Lastly, we demonstrate the detection of optical damage in a high-power laser system. The reliability of the object detector is demonstrated over 1000 laser shots in each application. Our study shows that deep object detection networks are suitable to assist online and offline experimental analysis, even with small training sets. We believe that the presented methodology is adaptable yet robust, and we encourage further applications in Hz-level or kHz-level high-power laser facilities regarding the control and diagnostic tools, especially for those involving image data.

Keywords: high repetition rate; laser–plasma accelerators; machine learning; object detection; optical diagnostics

1. Introduction

High-power laser systems with power reaching the petawatt level and repetition rate at a fraction of a hertz have emerged worldwide in the past few years[1–5]. With the fast development of high-repetition-rate operation capabilities in plasma targetry, high-power laser–plasma experiments can employ statistical methods that require a large number of shots. Studies for real-time optimization using evolutionary algorithms have been reported in recent years[6–11]. As the size of data to process has continued to increase, more advanced machine learning models have attracted increasing attention. By constructing predictive models, machine learning methods are employed to model the nonlinear, high-dimensional processes in high-power laser experiments. Various methods, including neural networks, Bayesian inference and decision trees, have been introduced for optimization tasks and physics interpretation[12–17]. Meanwhile, as the measurement and diagnostic tools evolve, digital imaging is playing an increasingly important role in experiments and, with it, machine learning methods to process image data.

Correspondence to: Jinpu Lin, Ludwig-Maximilians-Universität München, Am Coulombwall 1, 85748 Garching, Germany. Email: Lin.Jinpu@physik.uni-muenchen.de

In the case of a laser–plasma accelerator, image-based diagnostics can take a variety of forms, from the optical elements in the high-power laser facility, over shadowgraphy and interferometry of plasma dynamics, to scintillator signals generated by energetic electron or X-ray beams from the accelerator. In particular, the evolving structure of a plasma accelerator is challenging to visualize because of its microscopic size ($\sim 10^{-5}$ m) and its high velocity (approaching the speed of light). With the latest techniques, such as few-cycle shadowgraphy, taking snapshots of the plasma wake structure is enabled in femtosecond resolution over a range of picoseconds[18–20]. The latest generation of laboratory diagnostics for plasma structures is reviewed by Downer *et al.*[21].

In this paper, we demonstrate exemplary applications of an object detection network in the diagnostics in a high-power laser laboratory. We apply the object detector to few-cycle shadowgraphy of plasma waves, to an electron energy spectrometer and to detect optical damages in a high-power laser beamline. The results show that object detection enables possibilities in diagnostics and data analysis that have not yet been achieved using conventional methods. Moreover, due to the fast inference speed of the object detector, it paves the road towards real-time demonstration of such diagnostics during experiments.

1

https://doi.org/10.1017/hpl.2023.1 Published online by Cambridge University Press

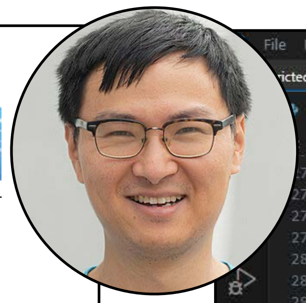

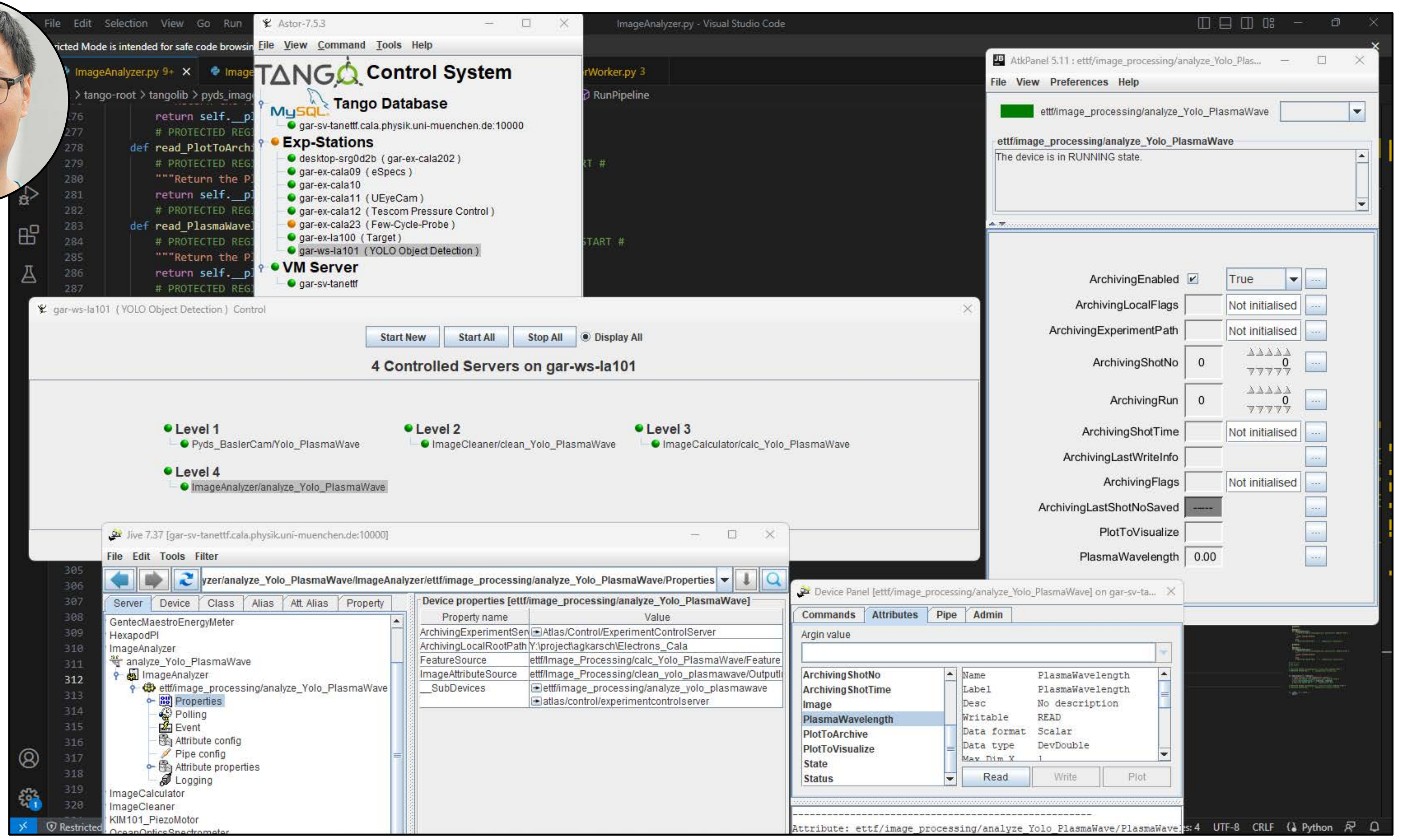

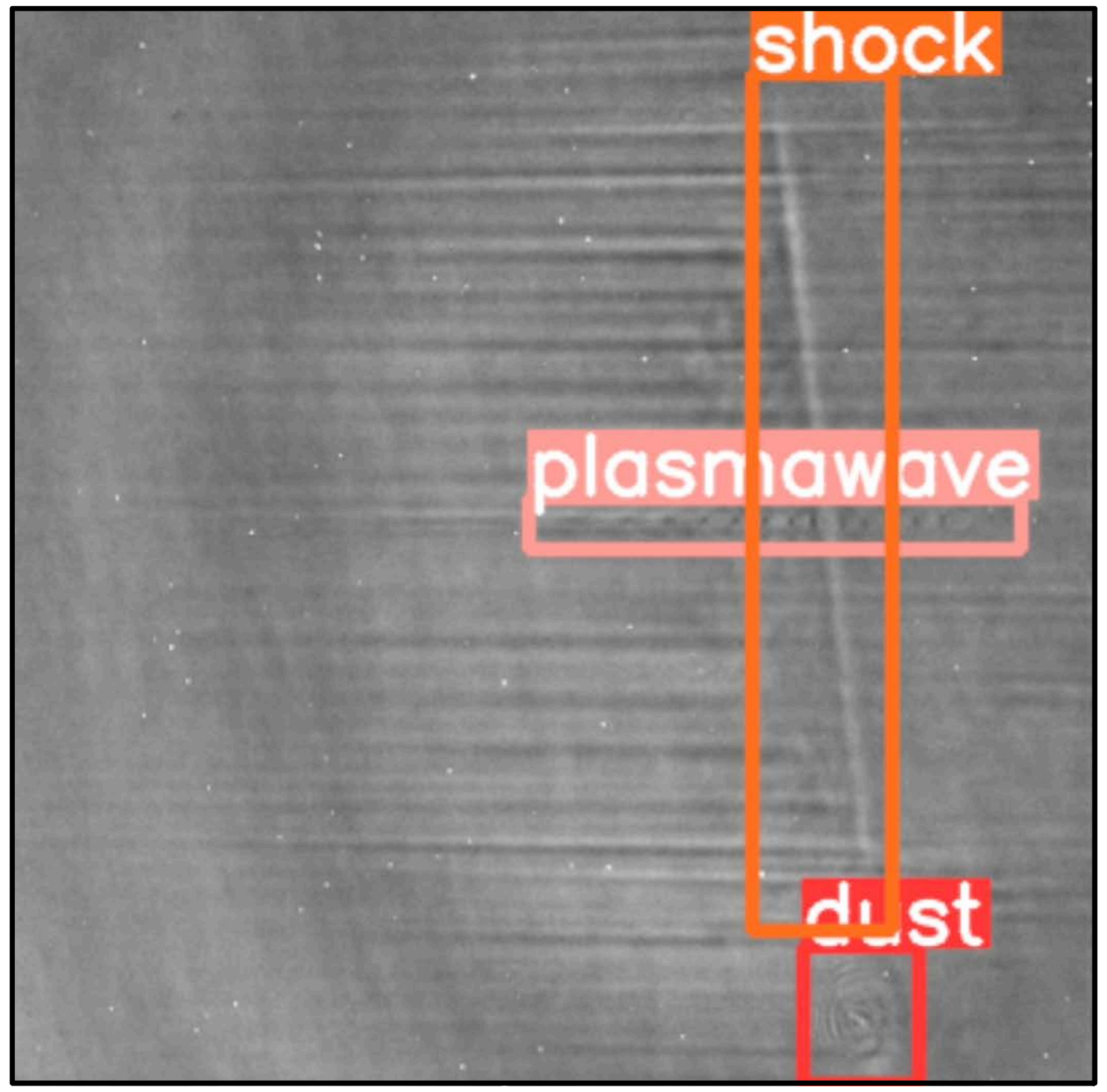

- Implemented in TANGO

  (get image from camera, remove noise, detect features, show results)

- Allows for live analysis during experiments

Phase III Custom-built methods

Example I

Spatio-Temporal Laser Pulse Characterization

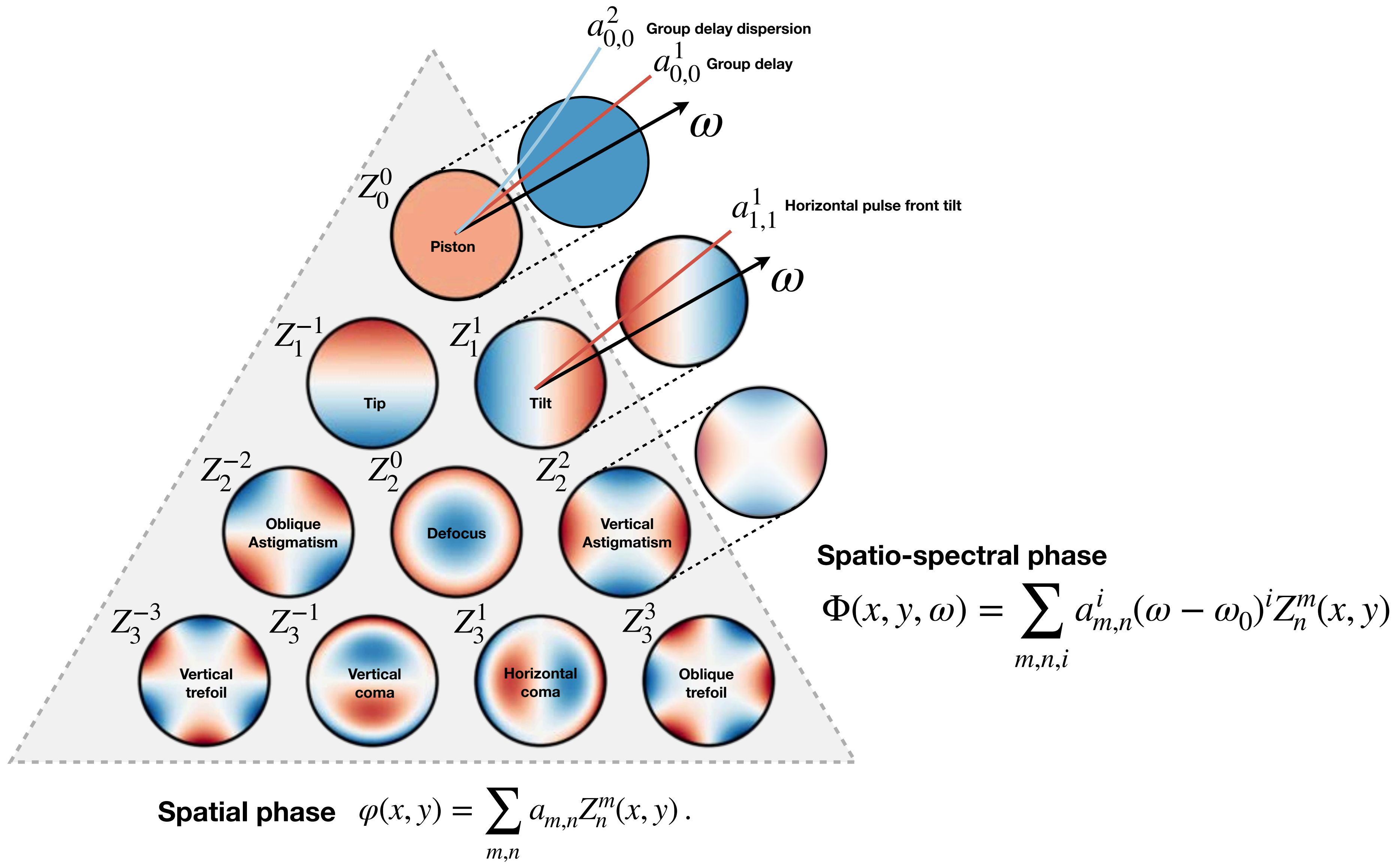

Example II

Laser-Accelerator Optimization

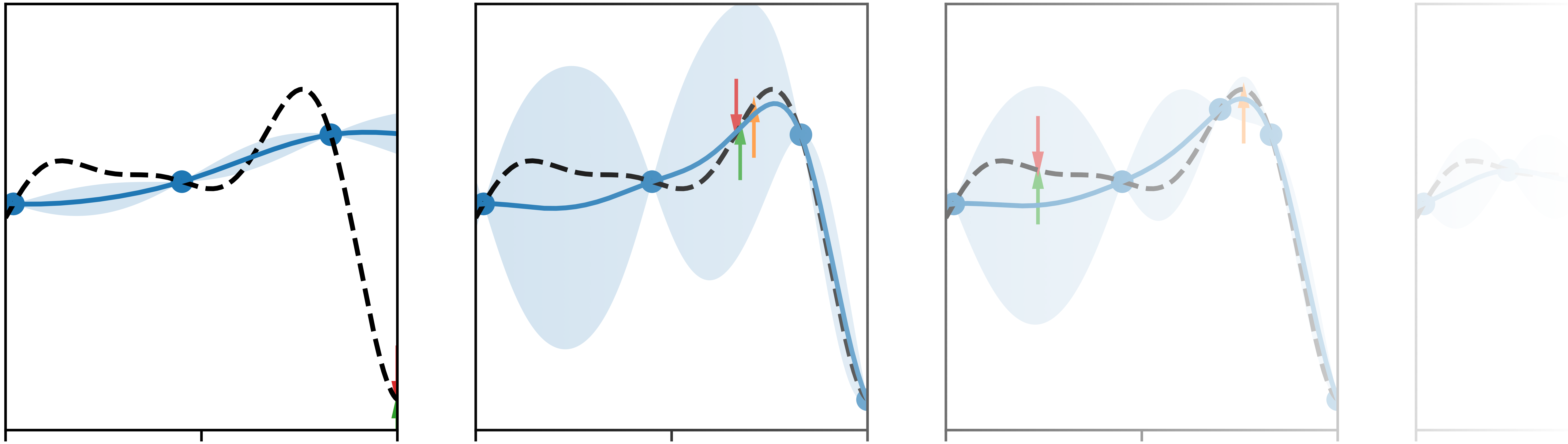

Ultra-intense laser characterization

3-D intensity distribution in time

Knowledge necessary for

- Highest peak-intensity
- Accurate simulations
- Spatio-temporal shaping (flying focus etc.)
- …

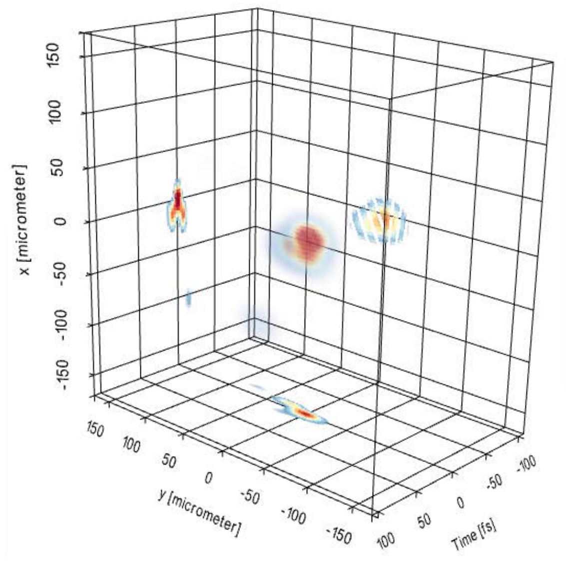

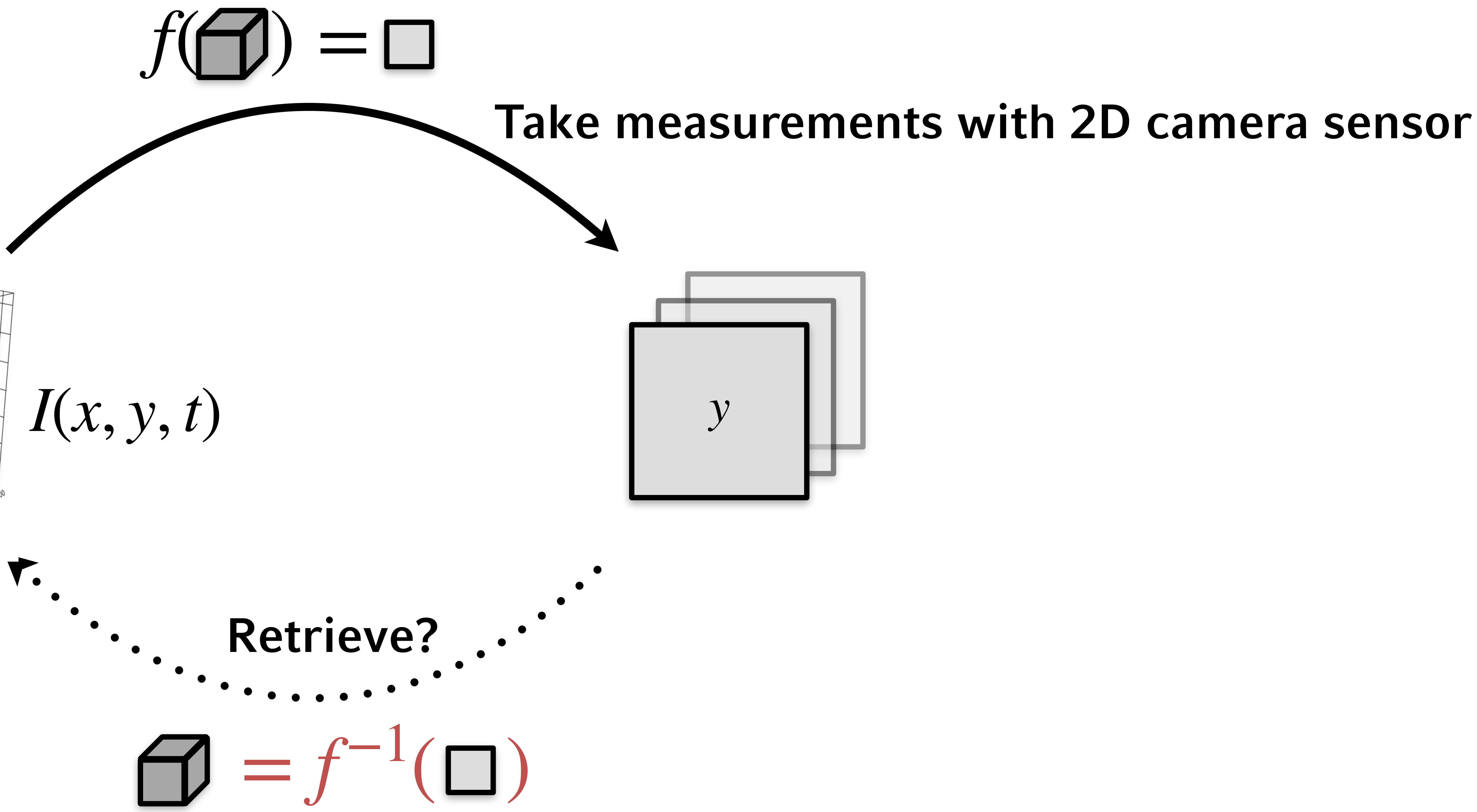

Ultra-intense laser characterization

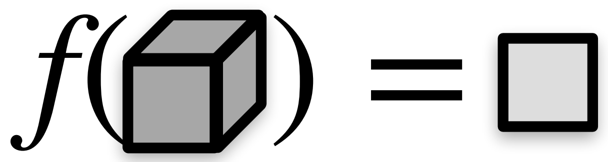

Take measurements with 2D camera sensor

3-D intensity distribution in time

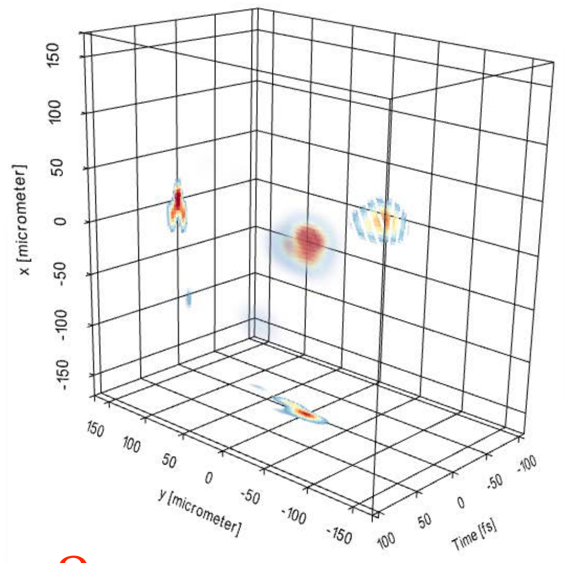

$I(x, y, t)$

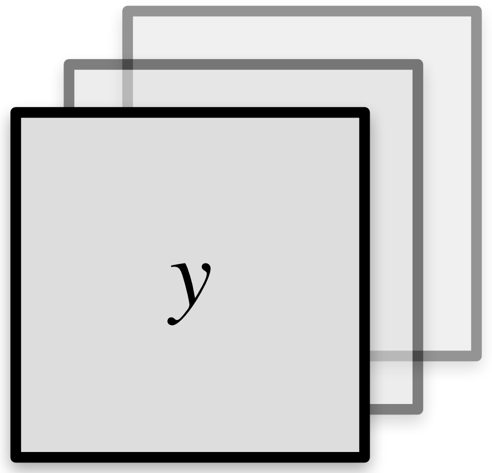

$n = n_x \times n_y \times n_\lambda$

$\sim 1000 \times 1000 \times 100 = 10^8$ voxels

Retrieve?

100 million voxels / parameters: Need <u>many</u> measurements (e.g. Fourier transform spectroscopy with >1000 2D measurements)

But are voxels really a good base function choice?

Ultra-intense laser characterization

Multi-spectral, modal reconstruction

$$I(x,y,t) = \|\mathscr{F}\left[\sqrt{I(x,y,\omega)} \cdot \exp\left(i\Phi(x,y,\omega)\right)\right]\|^2$$

This is the important part, describing how light of different color is focused!

$\Phi(x,y,\omega)$

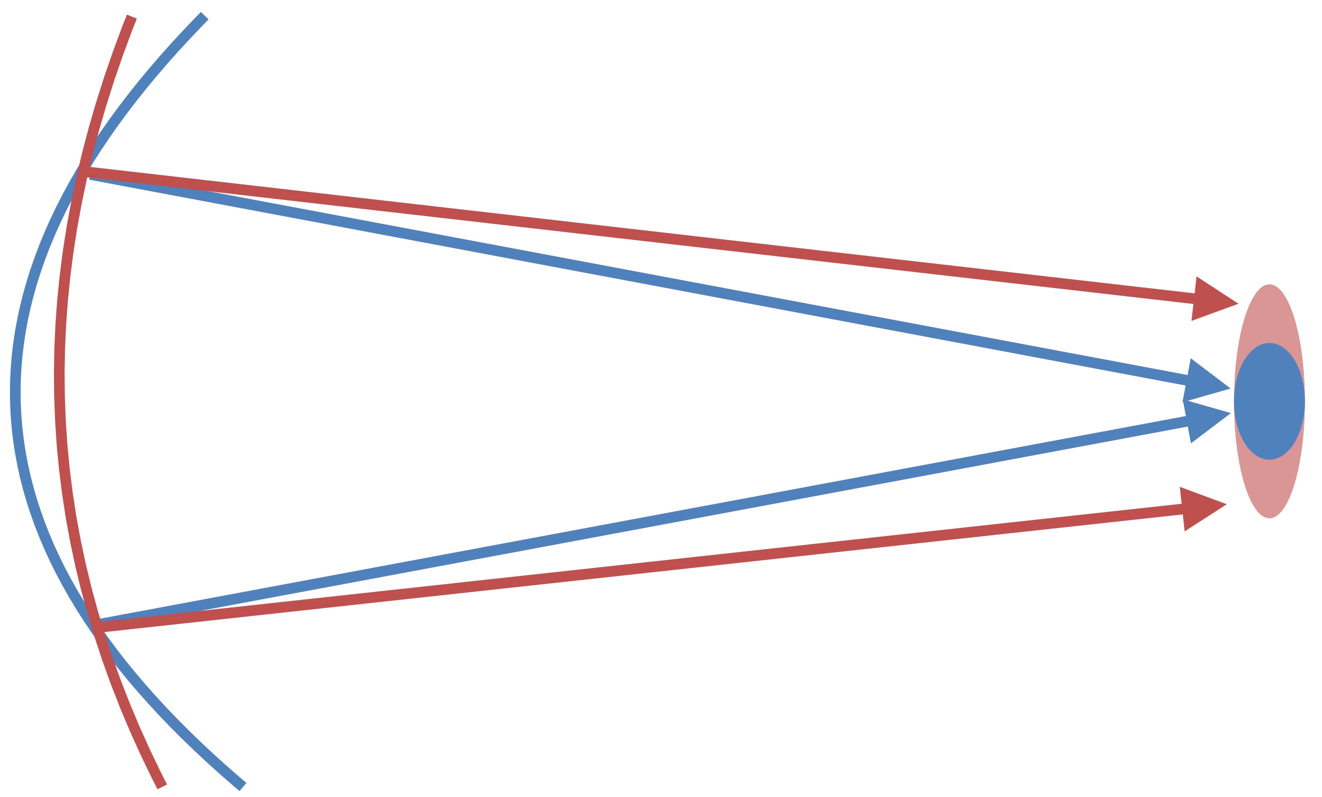

Ultra-intense laser characterization

Multi-spectral, modal reconstruction

$$I(x,y,t) = \|\mathscr{F}\left[\sqrt{I(x,y,\omega)} \cdot \exp\left(i\Phi(x,y,\omega)\right)\right]\|^2$$

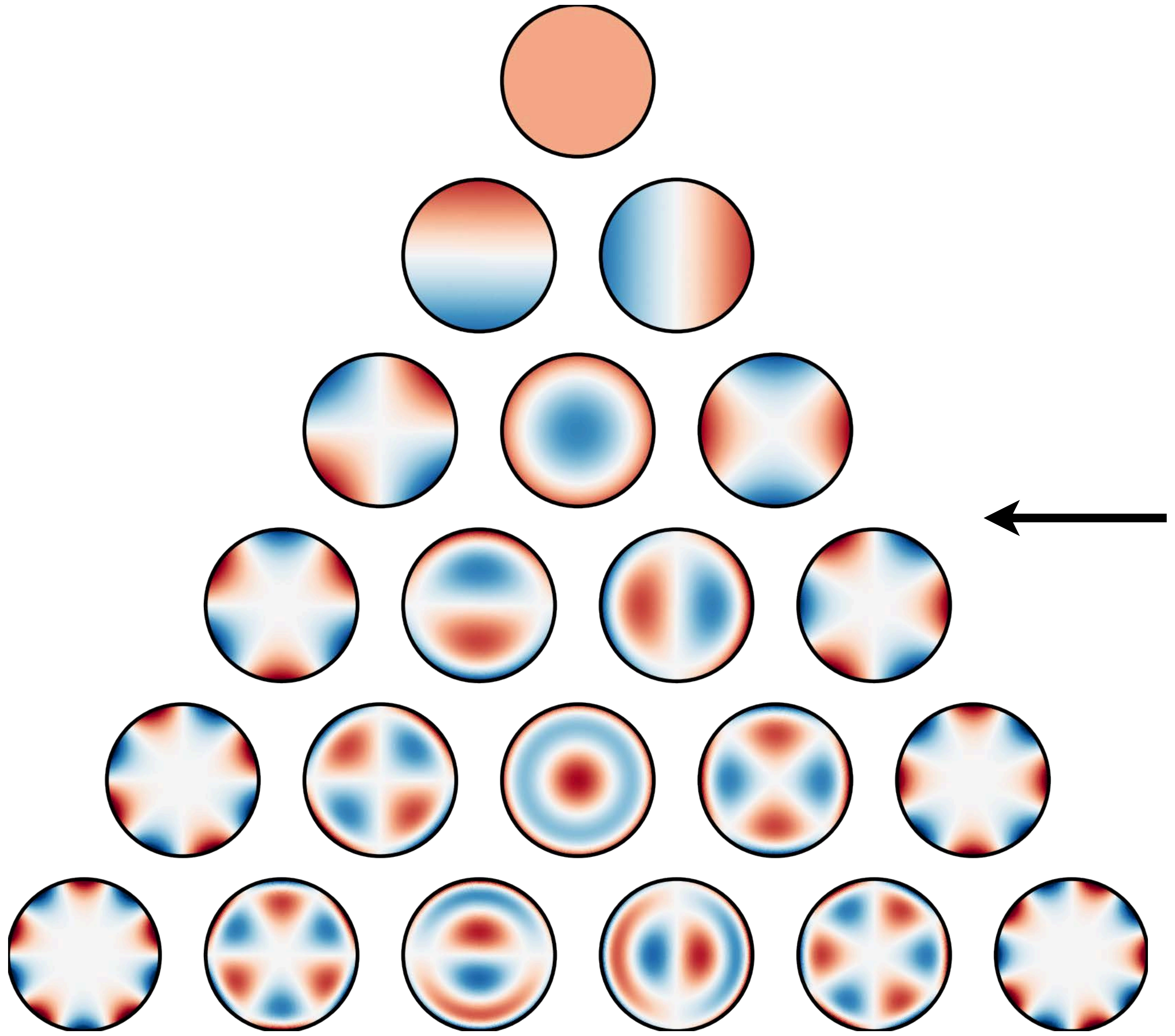

We know there is a very good base to describe phase:
Zernike polynomials

$$Z_n^m(\rho,\varphi) = R_n^m(\rho)\,\cos(m\,\varphi)$$

$$Z_n^{-m}(\rho,\varphi) = R_n^m(\rho)\,\sin(m\,\varphi),$$

Ultra-intense laser characterization

Multi-spectral, modal reconstruction

$$I(x,y,t) = \|\mathscr{F}\left[\sqrt{I(x,y,\omega)}\cdot\exp\left(i\Phi(x,y,\omega)\right)\right]\|^2$$

We also know there is a very good way to describe spectral phase: **Taylor expansion** (group delay, group delay dispersion, etc.)

Ultra-intense laser characterization

Multi-spectral, modal reconstruction

$$I(x,y,t) = \|\mathscr{F}\left[\sqrt{I(x,y,\omega)}\cdot \exp\left(i\Phi(x,y,\omega)\right)\right]\|^2$$

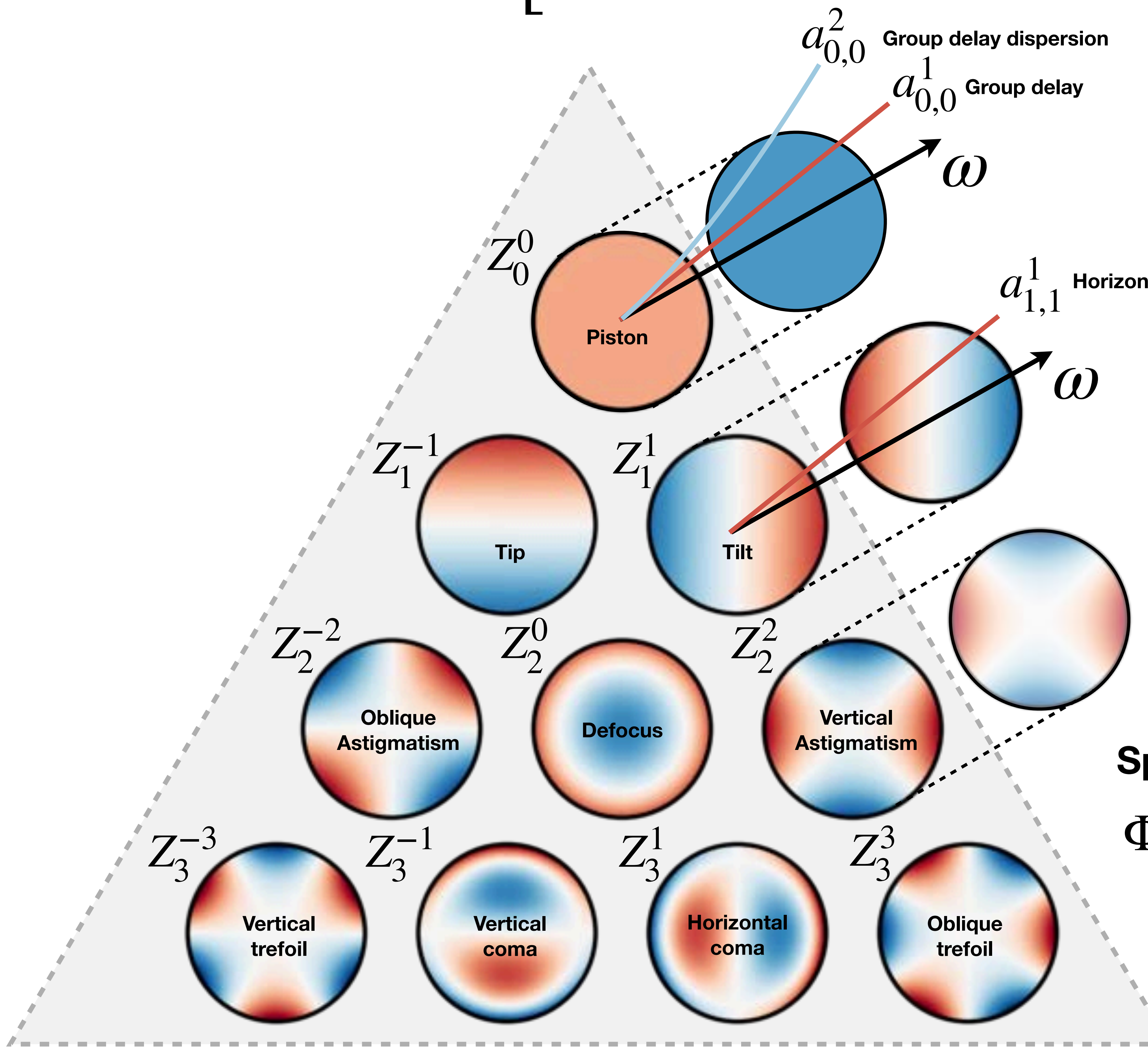

Can describe the **hyperspectral wavefront** using **Zernike-modes and Taylor-expansion in frequency**

Instead of > 1,000,000 voxels we only need to reconstruct dominant mode coefficients: Need less measurements

Spatio-spectral phase

$$\Phi(x,y,\omega) = \sum_{m,n,i} a^i_{m,n}(\omega-\omega_0)^i Z^m_n(x,y)$$

Spatial phase $\varphi(x,y) = \sum_{m,n} a_{m,n} Z^m_n(x,y)\,.$

Ultra-intense laser characterization

FALCON - Fast Acquisition of Laser Couplings using Narrowband Filters

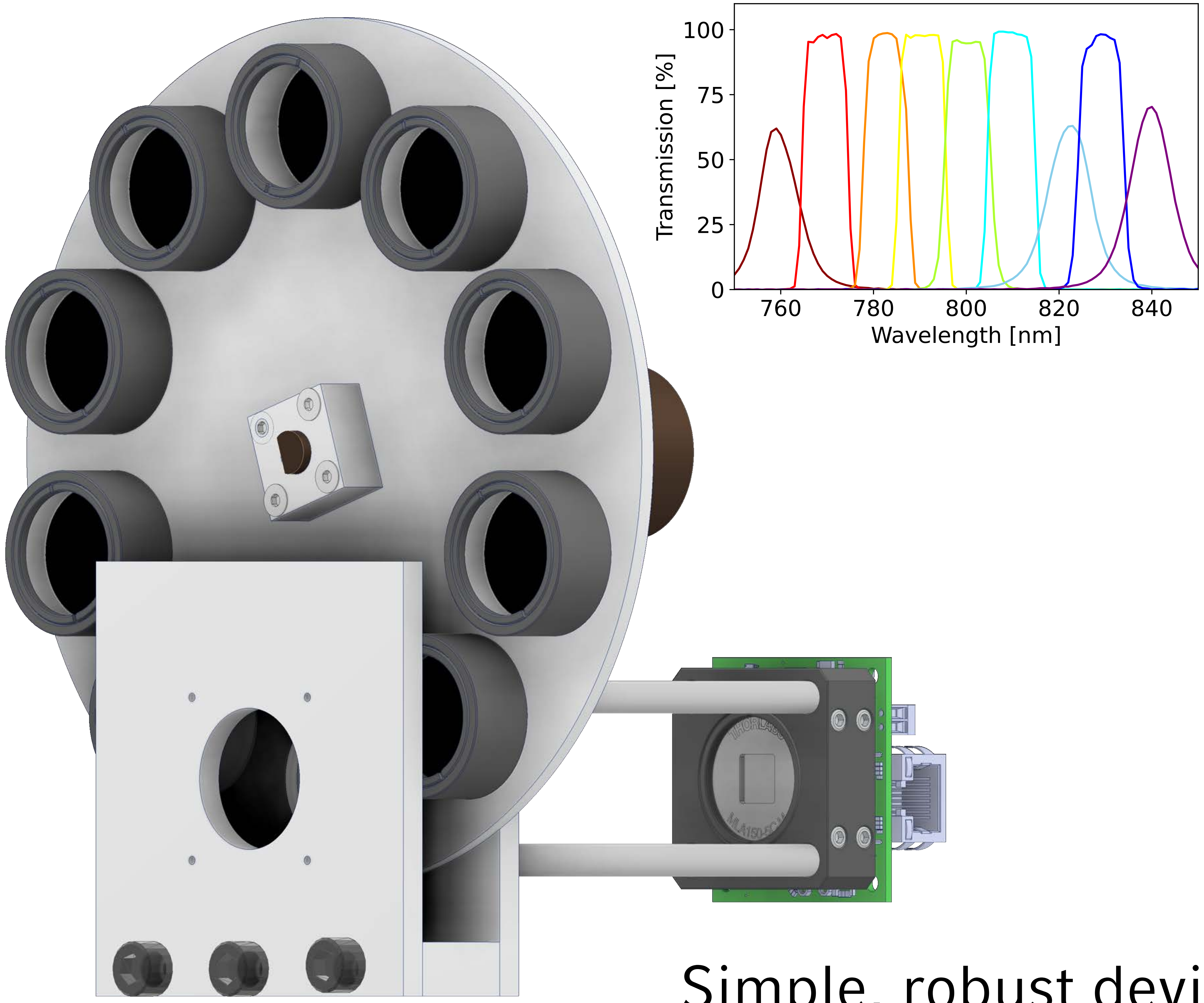

Simple, robust device

- N. Weiße, J. Esslinger et al. Measuring spatial-temporal couplings using modal multi-spectral wavefront reconstruction, Opt. Express 31, 19733-19745 (2023)

Ultra-intense laser characterization

FALCON - Fast Acquisition of Laser Couplings using Narrowband Filters

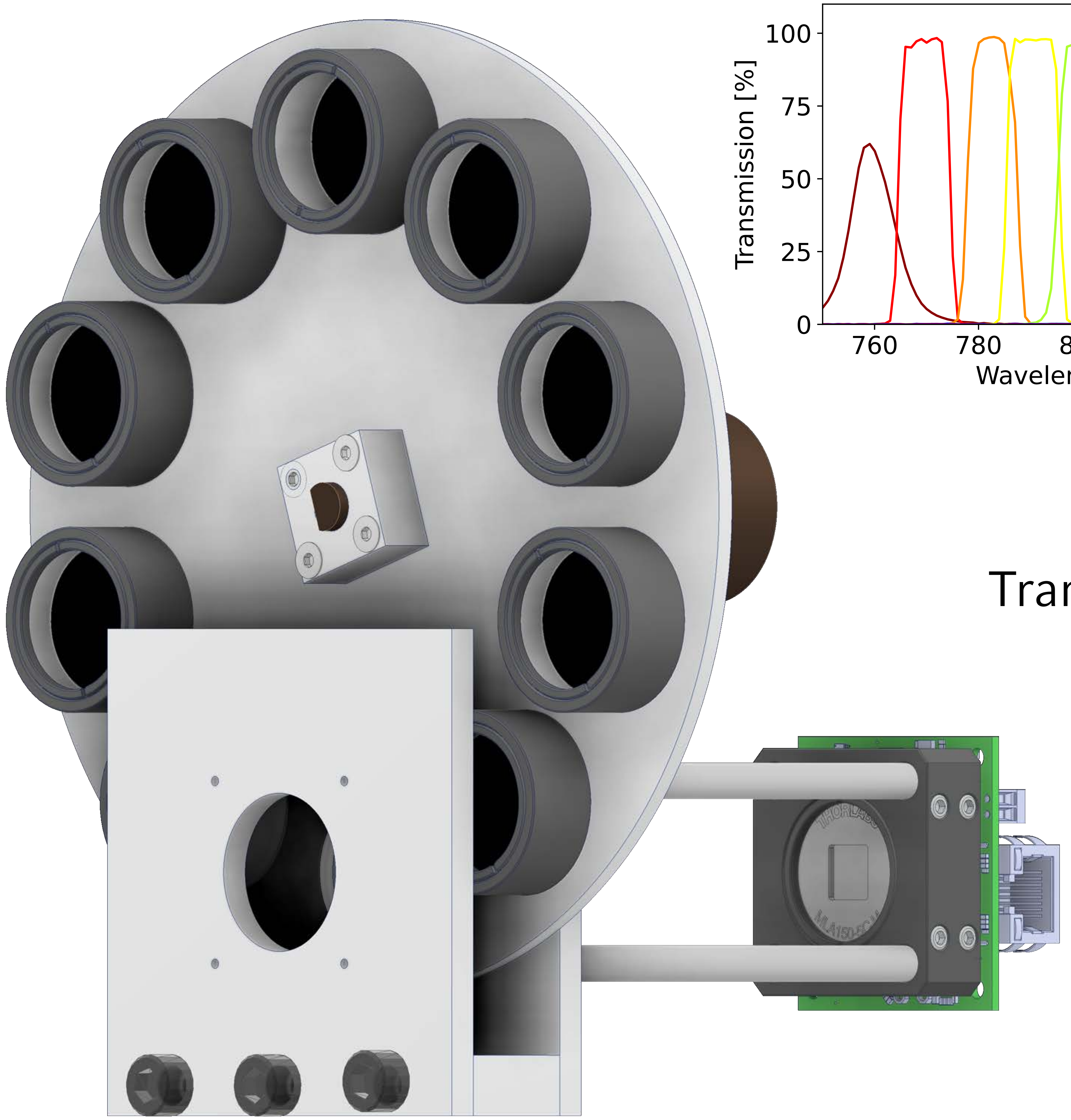

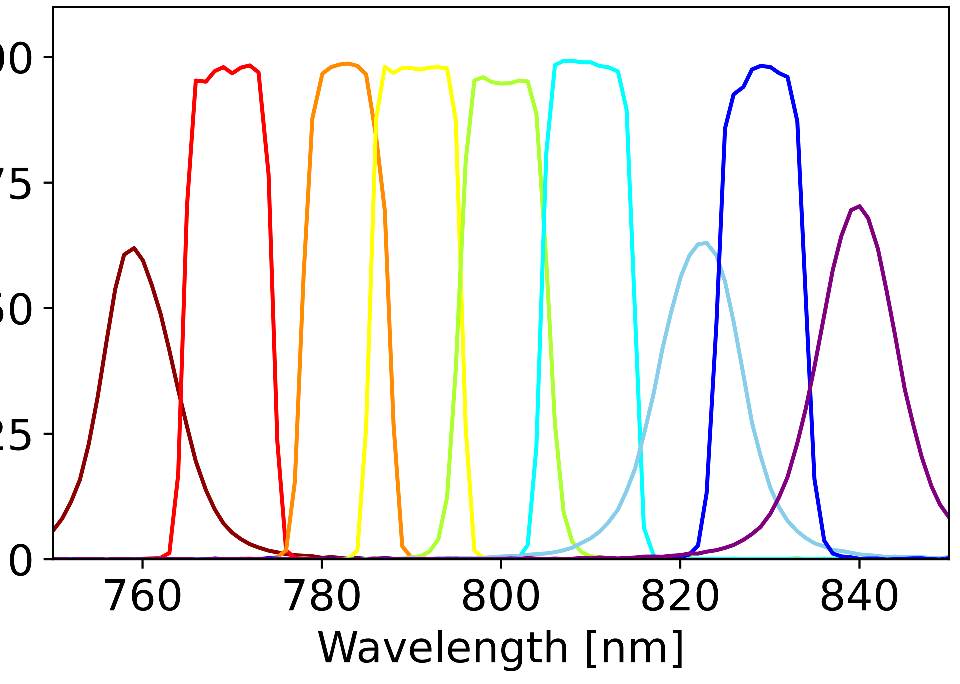

Translate into a forward problem

This is for a simple 2x2 lenslet SH detector

$$
\begin{pmatrix}
s_{x,\omega_1}(0,0)\\ s_{x,\omega_1}(0,1)\\ s_{x,\omega_1}(1,0)\\ s_{x,\omega_1}(1,1)\\
s_{y,\omega_1}(0,0)\\ s_{y,\omega_1}(0,1)\\ s_{y,\omega_1}(1,0)\\ s_{y,\omega_1}(1,1)\\
s_{x,\omega_2}(0,0)\\ s_{x,\omega_2}(0,1)\\ s_{x,\omega_2}(1,0)\\ s_{x,\omega_2}(1,1)\\
s_{y,\omega_2}(0,0)\\ s_{y,\omega_2}(0,1)\\ s_{y,\omega_2}(1,0)\\ s_{y,\omega_2}(1,1)
\end{pmatrix}
=
\begin{pmatrix}
\left.\frac{\mathrm{d}Z_1^{-1}}{\mathrm{d}x}\right|_{0,0} & \left.\frac{\mathrm{d}Z_1^{1}}{\mathrm{d}x}\right|_{0,0} & \left.\frac{\mathrm{d}Z_0^{0}}{\mathrm{d}x}\right|_{0,0}\tilde{\omega}_1^1 & \left.\frac{\mathrm{d}Z_1^{-1}}{\mathrm{d}x}\right|_{0,0}\tilde{\omega}_1^1 & \left.\frac{\mathrm{d}Z_1^{1}}{\mathrm{d}x}\right|_{0,0}\tilde{\omega}_1^1\\
\left.\frac{\mathrm{d}Z_1^{-1}}{\mathrm{d}x}\right|_{0,1} & \left.\frac{\mathrm{d}Z_1^{1}}{\mathrm{d}x}\right|_{0,1} & \left.\frac{\mathrm{d}Z_0^{0}}{\mathrm{d}x}\right|_{0,1}\tilde{\omega}_1^1 & \left.\frac{\mathrm{d}Z_1^{-1}}{\mathrm{d}x}\right|_{0,1}\tilde{\omega}_1^1 & \left.\frac{\mathrm{d}Z_1^{1}}{\mathrm{d}x}\right|_{0,1}\tilde{\omega}_1\\
\left.\frac{\mathrm{d}Z_1^{-1}}{\mathrm{d}x}\right|_{1,0} & \left.\frac{\mathrm{d}Z_1^{1}}{\mathrm{d}x}\right|_{1,0} & \left.\frac{\mathrm{d}Z_0^{0}}{\mathrm{d}x}\right|_{1,0}\tilde{\omega}_1^1 & \left.\frac{\mathrm{d}Z_1^{-1}}{\mathrm{d}x}\right|_{1,0}\tilde{\omega}_1^1 & \left.\frac{\mathrm{d}Z_1^{1}}{\mathrm{d}x}\right|_{1,0}\tilde{\omega}_1^1\\
\left.\frac{\mathrm{d}Z_1^{-1}}{\mathrm{d}x}\right|_{1,1} & \left.\frac{\mathrm{d}Z_1^{1}}{\mathrm{d}x}\right|_{1,1} & \left.\frac{\mathrm{d}Z_0^{0}}{\mathrm{d}x}\right|_{1,1}\tilde{\omega}_1^1 & \left.\frac{\mathrm{d}Z_1^{-1}}{\mathrm{d}x}\right|_{1,1}\tilde{\omega}_1^1 & \left.\frac{\mathrm{d}Z_1^{1}}{\mathrm{d}x}\right|_{1,1}\tilde{\omega}_1^1\\
\left.\frac{\mathrm{d}Z_1^{-1}}{\mathrm{d}y}\right|_{0,0} & \left.\frac{\mathrm{d}Z_1^{1}}{\mathrm{d}y}\right|_{0,0} & \left.\frac{\mathrm{d}Z_2^{-2}}{\mathrm{d}y}\right|_{0,0}\tilde{\omega}_1^1 & \left.\frac{\mathrm{d}Z_2^{0}}{\mathrm{d}y}\right|_{0,0}\tilde{\omega}_1^1 & \left.\frac{\mathrm{d}Z_2^{2}}{\mathrm{d}y}\right|_{0,0}\tilde{\omega}_1^1\\
\left.\frac{\mathrm{d}Z_1^{-1}}{\mathrm{d}y}\right|_{0,1} & \left.\frac{\mathrm{d}Z_1^{1}}{\mathrm{d}y}\right|_{0,1} & \left.\frac{\mathrm{d}Z_2^{-2}}{\mathrm{d}y}\right|_{0,1}\tilde{\omega}_1^1 & \left.\frac{\mathrm{d}Z_2^{0}}{\mathrm{d}y}\right|_{0,1}\tilde{\omega}_1^1 & \left.\frac{\mathrm{d}Z_2^{2}}{\mathrm{d}y}\right|_{0,1}\tilde{\omega}_1^1\\
\left.\frac{\mathrm{d}Z_1^{-1}}{\mathrm{d}y}\right|_{1,0} & \left.\frac{\mathrm{d}Z_1^{1}}{\mathrm{d}y}\right|_{1,0} & \left.\frac{\mathrm{d}Z_2^{-2}}{\mathrm{d}y}\right|_{1,0}\tilde{\omega}_1^1 & \left.\frac{\mathrm{d}Z_2^{0}}{\mathrm{d}y}\right|_{1,0}\tilde{\omega}_1^1 & \left.\frac{\mathrm{d}Z_2^{2}}{\mathrm{d}y}\right|_{1,0}\tilde{\omega}_1^1\\
\left.\frac{\mathrm{d}Z_1^{-1}}{\mathrm{d}y}\right|_{1,1} & \left.\frac{\mathrm{d}Z_1^{1}}{\mathrm{d}y}\right|_{1,1} & \left.\frac{\mathrm{d}Z_2^{-2}}{\mathrm{d}y}\right|_{1,1}\tilde{\omega}_1^1 & \left.\frac{\mathrm{d}Z_2^{0}}{\mathrm{d}y}\right|_{1,1}\tilde{\omega}_1^1 & \left.\frac{\mathrm{d}Z_2^{2}}{\mathrm{d}y}\right|_{1,1}\tilde{\omega}_1^1\\
\left.\frac{\mathrm{d}Z_1^{-1}}{\mathrm{d}x}\right|_{0,0} & \left.\frac{\mathrm{d}Z_1^{1}}{\mathrm{d}x}\right|_{0,0} & \left.\frac{\mathrm{d}Z_0^{0}}{\mathrm{d}x}\right|_{0,0}\tilde{\omega}_2^1 & \left.\frac{\mathrm{d}Z_1^{-1}}{\mathrm{d}x}\right|_{0,0}\tilde{\omega}_2^1 & \left.\frac{\mathrm{d}Z_1^{1}}{\mathrm{d}x}\right|_{0,0}\tilde{\omega}_2^1\\
\left.\frac{\mathrm{d}Z_1^{-1}}{\mathrm{d}x}\right|_{0,1} & \left.\frac{\mathrm{d}Z_1^{1}}{\mathrm{d}x}\right|_{0,1} & \left.\frac{\mathrm{d}Z_0^{0}}{\mathrm{d}x}\right|_{0,1}\tilde{\omega}_2^1 & \left.\frac{\mathrm{d}Z_1^{-1}}{\mathrm{d}x}\right|_{0,1}\tilde{\omega}_2^1 & \left.\frac{\mathrm{d}Z_1^{1}}{\mathrm{d}x}\right|_{0,1}\tilde{\omega}_2^1\\
\left.\frac{\mathrm{d}Z_1^{-1}}{\mathrm{d}x}\right|_{1,0} & \left.\frac{\mathrm{d}Z_1^{1}}{\mathrm{d}x}\right|_{1,0} & \left.\frac{\mathrm{d}Z_0^{0}}{\mathrm{d}x}\right|_{1,0}\tilde{\omega}_2^1 & \left.\frac{\mathrm{d}Z_1^{-1}}{\mathrm{d}x}\right|_{1,0}\tilde{\omega}_2^1 & \left.\frac{\mathrm{d}Z_1^{1}}{\mathrm{d}x}\right|_{1,0}\tilde{\omega}_2^1\\
\left.\frac{\mathrm{d}Z_1^{-1}}{\mathrm{d}x}\right|_{1,1} & \left.\frac{\mathrm{d}Z_1^{1}}{\mathrm{d}x}\right|_{1,1} & \left.\frac{\mathrm{d}Z_0^{0}}{\mathrm{d}x}\right|_{1,1}\tilde{\omega}_2^1 & \left.\frac{\mathrm{d}Z_1^{-1}}{\mathrm{d}x}\right|_{1,1}\tilde{\omega}_2^1 & \left.\frac{\mathrm{d}Z_1^{1}}{\mathrm{d}x}\right|_{1,1}\tilde{\omega}_2^1\\
\left.\frac{\mathrm{d}Z_1^{-1}}{\mathrm{d}y}\right|_{0,0} & \left.\frac{\mathrm{d}Z_1^{1}}{\mathrm{d}y}\right|_{0,0} & \left.\frac{\mathrm{d}Z_2^{-2}}{\mathrm{d}y}\right|_{0,0}\tilde{\omega}_2^1 & \left.\frac{\mathrm{d}Z_2^{0}}{\mathrm{d}y}\right|_{0,0}\tilde{\omega}_2^1 & \left.\frac{\mathrm{d}Z_2^{2}}{\mathrm{d}y}\right|_{0,0}\tilde{\omega}_2^1\\
\left.\frac{\mathrm{d}Z_1^{-1}}{\mathrm{d}y}\right|_{0,1} & \left.\frac{\mathrm{d}Z_1^{1}}{\mathrm{d}y}\right|_{0,1} & \left.\frac{\mathrm{d}Z_2^{-2}}{\mathrm{d}y}\right|_{0,1}\tilde{\omega}_2^1 & \left.\frac{\mathrm{d}Z_2^{0}}{\mathrm{d}y}\right|_{0,1}\tilde{\omega}_2^1 & \left.\frac{\mathrm{d}Z_2^{2}}{\mathrm{d}y}\right|_{0,1}\tilde{\omega}_2^1\\
\left.\frac{\mathrm{d}Z_1^{-1}}{\mathrm{d}y}\right|_{1,0} & \left.\frac{\mathrm{d}Z_1^{1}}{\mathrm{d}y}\right|_{1,0} & \left.\frac{\mathrm{d}Z_2^{-2}}{\mathrm{d}y}\right|_{1,0}\tilde{\omega}_2^1 & \left.\frac{\mathrm{d}Z_2^{0}}{\mathrm{d}y}\right|_{1,0}\tilde{\omega}_2^1 & \left.\frac{\mathrm{d}Z_2^{2}}{\mathrm{d}y}\right|_{1,0}\tilde{\omega}_2^1\\
\left.\frac{\mathrm{d}Z_1^{-1}}{\mathrm{d}y}\right|_{1,1} & \left.\frac{\mathrm{d}Z_1^{1}}{\mathrm{d}y}\right|_{1,1} & \left.\frac{\mathrm{d}Z_2^{-2}}{\mathrm{d}y}\right|_{1,1}\tilde{\omega}_2^1 & \left.\frac{\mathrm{d}Z_2^{0}}{\mathrm{d}y}\right|_{1,1}\tilde{\omega}_2^1 & \left.\frac{\mathrm{d}Z_2^{2}}{\mathrm{d}y}\right|_{1,1}\tilde{\omega}_2^1
\end{pmatrix}
\cdot
\begin{pmatrix}
a_{0,0}^0\\ a_{1,-1}^0\\ a_{1,1}^0\\ a_{0,0}^1\\ a_{1,-1}^1\\ a_{1,1}^1
\end{pmatrix}
$$

- N. Weiße, J. Esslinger et al. Measuring spatial-temporal couplings using modal multi-spectral wavefront reconstruction, Opt. Express 31, 19733-19745 (2023)

Ultra-intense laser characterization

FALCON - Fast Acquisition of Laser Couplings using Narrowband Filters

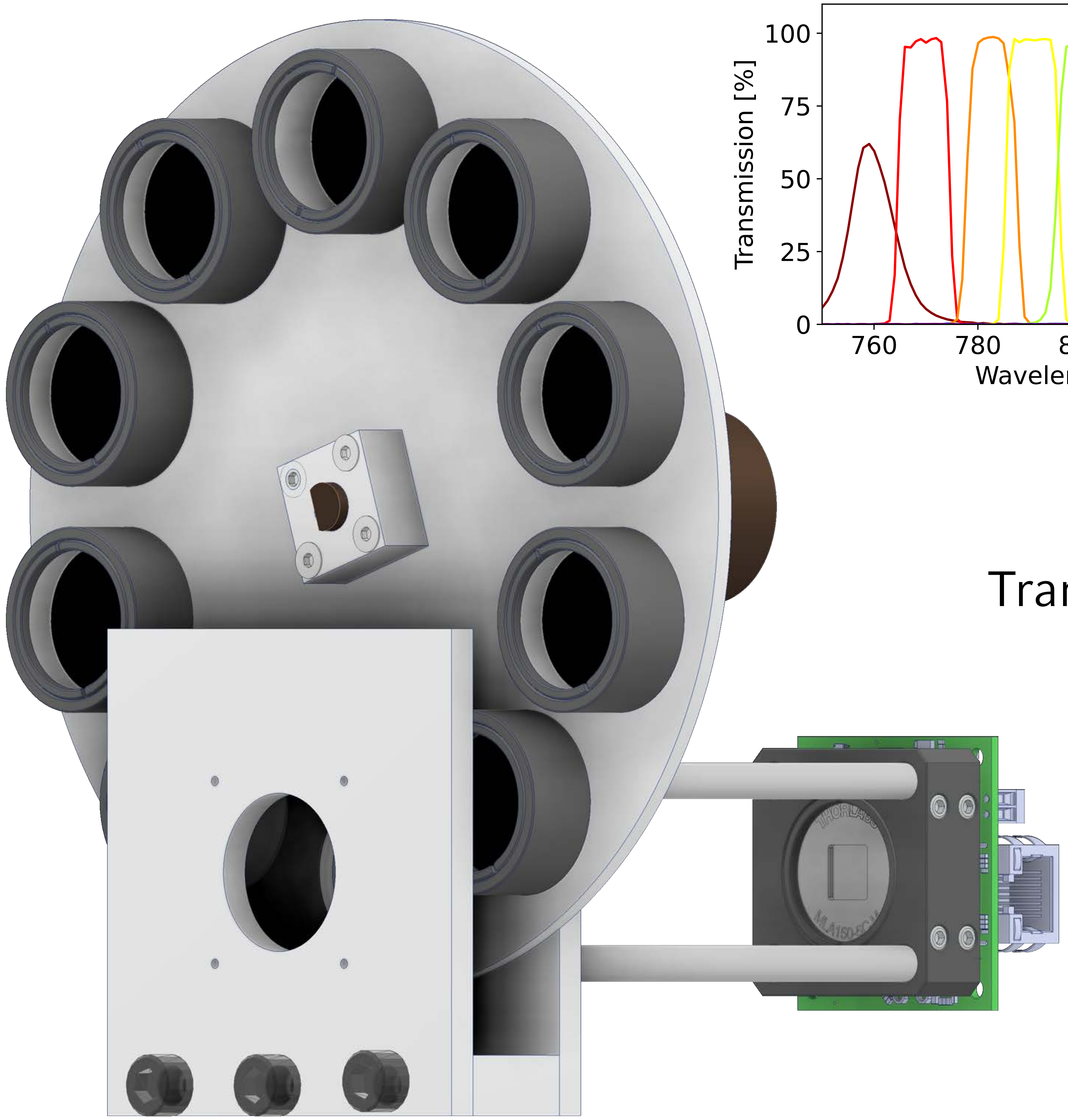

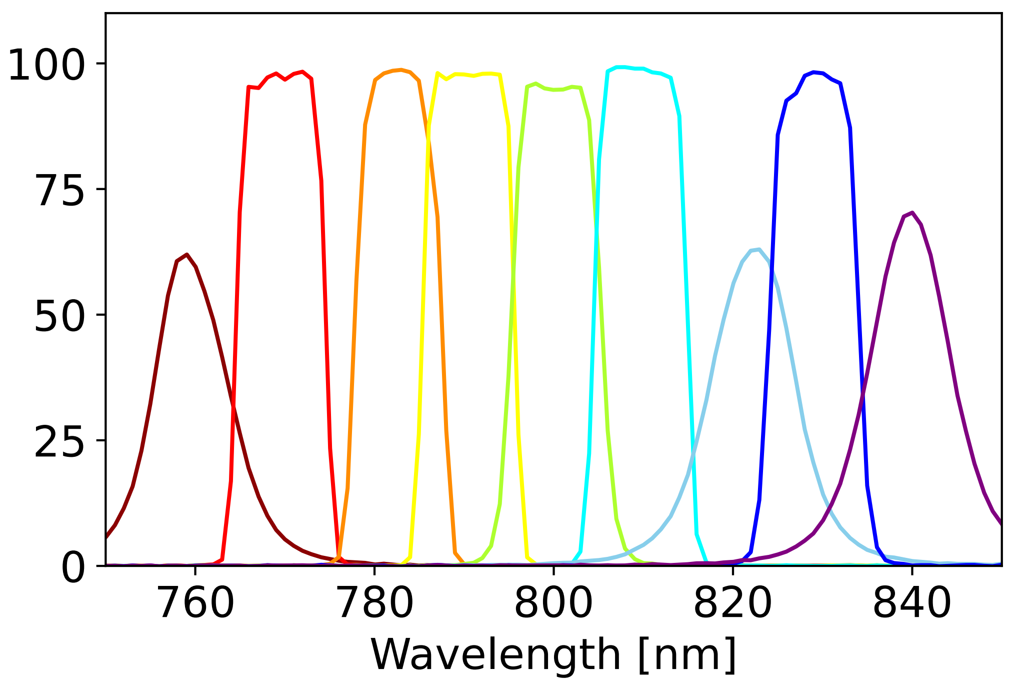

$$
\begin{pmatrix}
s_{x,\omega_1}(0,0)\\ s_{x,\omega_1}(0,1)\\ s_{x,\omega_1}(1,0)\\ s_{x,\omega_1}(1,1)\\ s_{y,\omega_1}(0,0)\\ s_{y,\omega_1}(0,1)\\ s_{y,\omega_1}(1,0)\\ s_{y,\omega_1}(1,1)\\ s_{x,\omega_2}(0,0)\\ s_{x,\omega_2}(0,1)\\ s_{x,\omega_2}(1,0)\\ s_{x,\omega_2}(1,1)\\ s_{y,\omega_2}(0,0)\\ s_{y,\omega_2}(0,1)\\ s_{y,\omega_2}(1,0)\\ s_{y,\omega_2}(1,1)
\end{pmatrix}
=
\begin{pmatrix}
\left.\frac{\mathrm{d}Z_1^{-1}}{\mathrm{d}x}\right|_{0,0} & \left.\frac{\mathrm{d}Z_1^{1}}{\mathrm{d}x}\right|_{0,0} & \left.\frac{\mathrm{d}Z_0^{0}}{\mathrm{d}x}\right|_{0,0}\tilde{\omega}_1^1 & \left.\frac{\mathrm{d}Z_1^{-1}}{\mathrm{d}x}\right|_{0,0}\tilde{\omega}_1^1 & \left.\frac{\mathrm{d}Z_1^{1}}{\mathrm{d}x}\right|_{0,0}\tilde{\omega}_1^1 \\
\left.\frac{\mathrm{d}Z_1^{-1}}{\mathrm{d}x}\right|_{0,1} & \left.\frac{\mathrm{d}Z_1^{1}}{\mathrm{d}x}\right|_{0,1} & \left.\frac{\mathrm{d}Z_0^{0}}{\mathrm{d}x}\right|_{0,1}\tilde{\omega}_1^1 & \left.\frac{\mathrm{d}Z_1^{-1}}{\mathrm{d}x}\right|_{0,1}\tilde{\omega}_1^1 & \left.\frac{\mathrm{d}Z_1^{1}}{\mathrm{d}x}\right|_{0,1}\tilde{\omega}_1 \\
\left.\frac{\mathrm{d}Z_1^{-1}}{\mathrm{d}x}\right|_{1,0} & \left.\frac{\mathrm{d}Z_1^{1}}{\mathrm{d}x}\right|_{1,0} & \left.\frac{\mathrm{d}Z_0^{0}}{\mathrm{d}x}\right|_{1,0}\tilde{\omega}_1^1 & \left.\frac{\mathrm{d}Z_1^{-1}}{\mathrm{d}x}\right|_{1,0}\tilde{\omega}_1^1 & \left.\frac{\mathrm{d}Z_1^{1}}{\mathrm{d}x}\right|_{1,0}\tilde{\omega}_1^1 \\
\left.\frac{\mathrm{d}Z_1^{-1}}{\mathrm{d}x}\right|_{1,1} & \left.\frac{\mathrm{d}Z_1^{1}}{\mathrm{d}x}\right|_{1,1} & \left.\frac{\mathrm{d}Z_0^{0}}{\mathrm{d}x}\right|_{1,1}\tilde{\omega}_1^1 & \left.\frac{\mathrm{d}Z_1^{-1}}{\mathrm{d}x}\right|_{1,1}\tilde{\omega}_1^1 & \left.\frac{\mathrm{d}Z_1^{1}}{\mathrm{d}x}\right|_{1,1}\tilde{\omega}_1^1 \\
\left.\frac{\mathrm{d}Z_1^{-1}}{\mathrm{d}y}\right|_{0,0} & \left.\frac{\mathrm{d}Z_1^{1}}{\mathrm{d}y}\right|_{0,0} & \left.\frac{\mathrm{d}Z_2^{-2}}{\mathrm{d}y}\right|_{0,0}\tilde{\omega}_1^1 & \left.\frac{\mathrm{d}Z_2^{0}}{\mathrm{d}y}\right|_{0,0}\tilde{\omega}_1^1 & \left.\frac{\mathrm{d}Z_2^{2}}{\mathrm{d}y}\right|_{0,0}\tilde{\omega}_1^1 \\
\left.\frac{\mathrm{d}Z_1^{-1}}{\mathrm{d}y}\right|_{0,1} & \left.\frac{\mathrm{d}Z_1^{1}}{\mathrm{d}y}\right|_{0,1} & \left.\frac{\mathrm{d}Z_2^{-2}}{\mathrm{d}y}\right|_{0,1}\tilde{\omega}_1^1 & \left.\frac{\mathrm{d}Z_2^{0}}{\mathrm{d}y}\right|_{0,1}\tilde{\omega}_1^1 & \left.\frac{\mathrm{d}Z_2^{2}}{\mathrm{d}y}\right|_{0,1}\tilde{\omega}_1^1 \\
\left.\frac{\mathrm{d}Z_1^{-1}}{\mathrm{d}y}\right|_{1,0} & \left.\frac{\mathrm{d}Z_1^{1}}{\mathrm{d}y}\right|_{1,0} & \left.\frac{\mathrm{d}Z_2^{-2}}{\mathrm{d}y}\right|_{1,0}\tilde{\omega}_1^1 & \left.\frac{\mathrm{d}Z_2^{0}}{\mathrm{d}y}\right|_{1,0}\tilde{\omega}_1^1 & \left.\frac{\mathrm{d}Z_2^{2}}{\mathrm{d}y}\right|_{1,0}\tilde{\omega}_1^1 \\
\left.\frac{\mathrm{d}Z_1^{-1}}{\mathrm{d}y}\right|_{1,1} & \left.\frac{\mathrm{d}Z_1^{1}}{\mathrm{d}y}\right|_{1,1} & \left.\frac{\mathrm{d}Z_2^{-2}}{\mathrm{d}y}\right|_{1,1}\tilde{\omega}_1^1 & \left.\frac{\mathrm{d}Z_2^{0}}{\mathrm{d}y}\right|_{1,1}\tilde{\omega}_1^1 & \left.\frac{\mathrm{d}Z_2^{2}}{\mathrm{d}y}\right|_{1,1}\tilde{\omega}_1^1 \\
\left.\frac{\mathrm{d}Z_1^{-1}}{\mathrm{d}x}\right|_{0,0} & \left.\frac{\mathrm{d}Z_1^{1}}{\mathrm{d}x}\right|_{0,0} & \left.\frac{\mathrm{d}Z_0^{0}}{\mathrm{d}x}\right|_{0,0}\tilde{\omega}_2^1 & \left.\frac{\mathrm{d}Z_1^{-1}}{\mathrm{d}x}\right|_{0,0}\tilde{\omega}_2^1 & \left.\frac{\mathrm{d}Z_1^{1}}{\mathrm{d}x}\right|_{0,0}\tilde{\omega}_2^1 \\
\left.\frac{\mathrm{d}Z_1^{-1}}{\mathrm{d}x}\right|_{0,1} & \left.\frac{\mathrm{d}Z_1^{1}}{\mathrm{d}x}\right|_{0,1} & \left.\frac{\mathrm{d}Z_0^{0}}{\mathrm{d}x}\right|_{0,1}\tilde{\omega}_2^1 & \left.\frac{\mathrm{d}Z_1^{-1}}{\mathrm{d}x}\right|_{0,1}\tilde{\omega}_2^1 & \left.\frac{\mathrm{d}Z_1^{1}}{\mathrm{d}x}\right|_{0,1}\tilde{\omega}_2^1 \\
\left.\frac{\mathrm{d}Z_1^{-1}}{\mathrm{d}x}\right|_{1,0} & \left.\frac{\mathrm{d}Z_1^{1}}{\mathrm{d}x}\right|_{1,0} & \left.\frac{\mathrm{d}Z_0^{0}}{\mathrm{d}x}\right|_{1,0}\tilde{\omega}_2^1 & \left.\frac{\mathrm{d}Z_1^{-1}}{\mathrm{d}x}\right|_{1,0}\tilde{\omega}_2^1 & \left.\frac{\mathrm{d}Z_1^{1}}{\mathrm{d}x}\right|_{1,0}\tilde{\omega}_2^1 \\
\left.\frac{\mathrm{d}Z_1^{-1}}{\mathrm{d}x}\right|_{1,1} & \left.\frac{\mathrm{d}Z_1^{1}}{\mathrm{d}x}\right|_{1,1} & \left.\frac{\mathrm{d}Z_0^{0}}{\mathrm{d}x}\right|_{1,1}\tilde{\omega}_2^1 & \left.\frac{\mathrm{d}Z_1^{-1}}{\mathrm{d}x}\right|_{1,1}\tilde{\omega}_2^1 & \left.\frac{\mathrm{d}Z_1^{1}}{\mathrm{d}x}\right|_{1,1}\tilde{\omega}_2^1 \\
\left.\frac{\mathrm{d}Z_1^{-1}}{\mathrm{d}y}\right|_{0,0} & \left.\frac{\mathrm{d}Z_1^{1}}{\mathrm{d}y}\right|_{0,0} & \left.\frac{\mathrm{d}Z_2^{-2}}{\mathrm{d}y}\right|_{0,0}\tilde{\omega}_2^1 & \left.\frac{\mathrm{d}Z_2^{0}}{\mathrm{d}y}\right|_{0,0}\tilde{\omega}_2^1 & \left.\frac{\mathrm{d}Z_2^{2}}{\mathrm{d}y}\right|_{0,0}\tilde{\omega}_2^1 \\
\left.\frac{\mathrm{d}Z_1^{-1}}{\mathrm{d}y}\right|_{0,1} & \left.\frac{\mathrm{d}Z_1^{1}}{\mathrm{d}y}\right|_{0,1} & \left.\frac{\mathrm{d}Z_2^{-2}}{\mathrm{d}y}\right|_{0,1}\tilde{\omega}_2^1 & \left.\frac{\mathrm{d}Z_2^{0}}{\mathrm{d}y}\right|_{0,1}\tilde{\omega}_2^1 & \left.\frac{\mathrm{d}Z_2^{2}}{\mathrm{d}y}\right|_{0,1}\tilde{\omega}_2^1 \\
\left.\frac{\mathrm{d}Z_1^{-1}}{\mathrm{d}y}\right|_{1,0} & \left.\frac{\mathrm{d}Z_1^{1}}{\mathrm{d}y}\right|_{1,0} & \left.\frac{\mathrm{d}Z_2^{-2}}{\mathrm{d}y}\right|_{1,0}\tilde{\omega}_2^1 & \left.\frac{\mathrm{d}Z_2^{0}}{\mathrm{d}y}\right|_{1,0}\tilde{\omega}_2^1 & \left.\frac{\mathrm{d}Z_2^{2}}{\mathrm{d}y}\right|_{1,0}\tilde{\omega}_2^1 \\
\left.\frac{\mathrm{d}Z_1^{-1}}{\mathrm{d}y}\right|_{1,1} & \left.\frac{\mathrm{d}Z_1^{1}}{\mathrm{d}y}\right|_{1,1} & \left.\frac{\mathrm{d}Z_2^{-2}}{\mathrm{d}y}\right|_{1,1}\tilde{\omega}_2^1 & \left.\frac{\mathrm{d}Z_2^{0}}{\mathrm{d}y}\right|_{1,1}\tilde{\omega}_2^1 & \left.\frac{\mathrm{d}Z_2^{2}}{\mathrm{d}y}\right|_{1,1}\tilde{\omega}_2^1
\end{pmatrix}
\cdot
\begin{pmatrix}
a_{0,0}^0\\ a_{1,-1}^0\\ a_{1,1}^0\\ a_{0,0}^1\\ a_{1,-1}^1\\ a_{1,1}^1
\end{pmatrix}
$$

Translate into a forward problem

Penrose pseudo-inverse calculation (basically realtime)

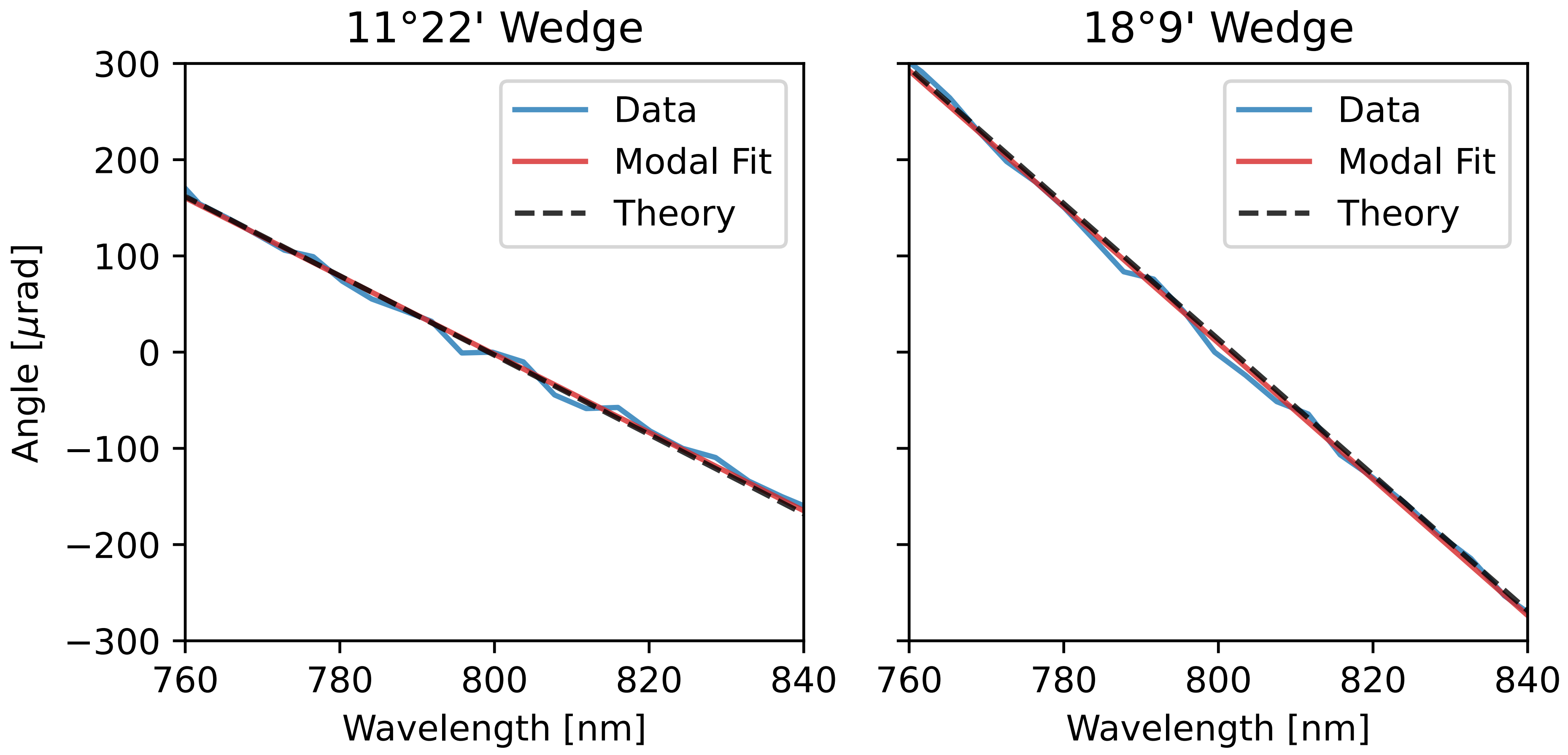

- N. Weiße, J. Esslinger et al. Measuring spatial-temporal couplings using modal multi-spectral wavefront reconstruction, Opt. Express 31, 19733-19745 (2023)

Ultra-intense laser characterization

Measurement of STCs of the ATLAS petawatt laser

- Full measurement takes ~ 1 minute (9 wavelengths, 5 shots each)
- Measurement shows couplings in ATLAS are < λ/10 between 780 - 820 nm
- FALCON measurement now routinely performed every day after focus measurements

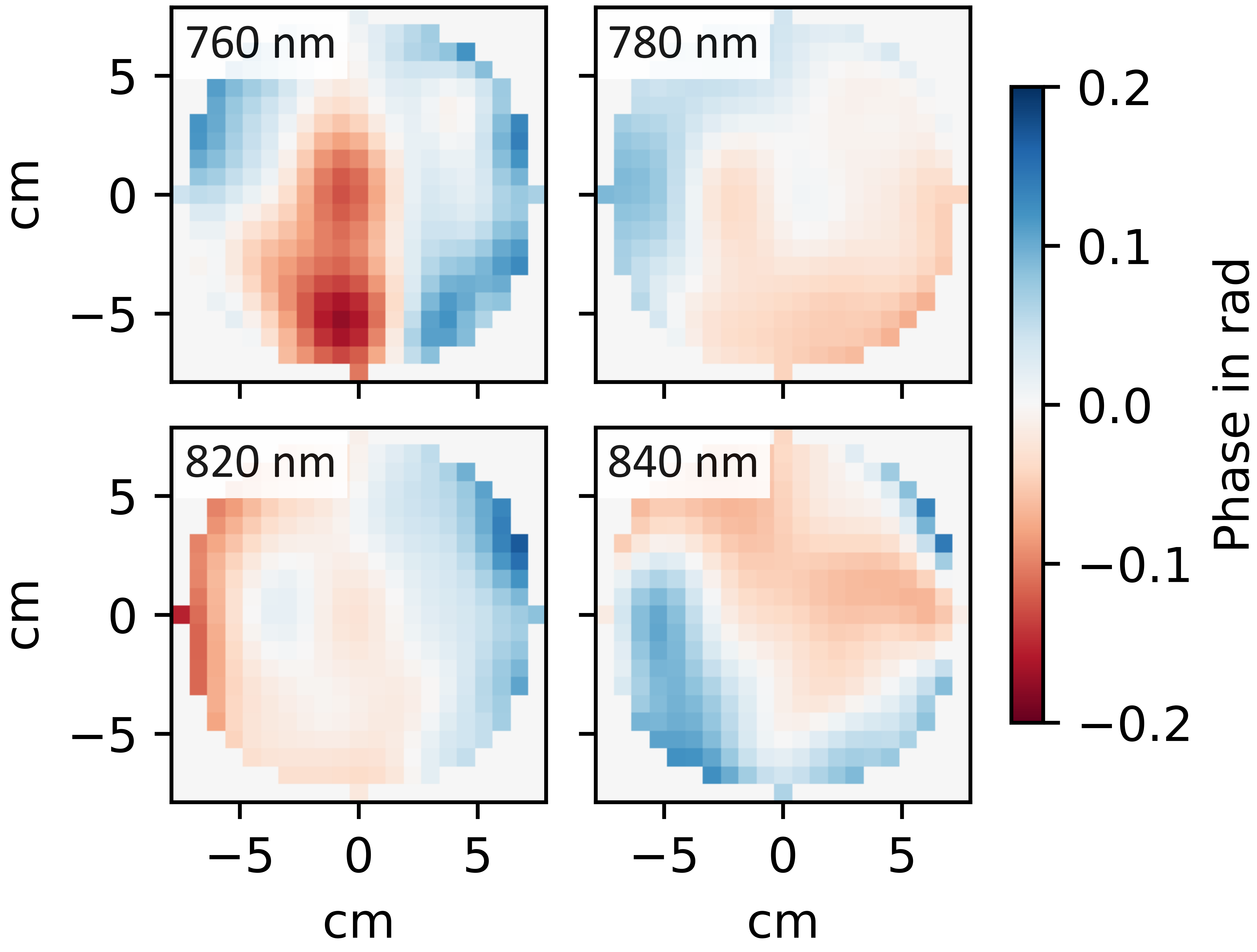

- N. Weiße, J. Esslinger et al. Measuring spatial-temporal couplings using modal multi-spectral wavefront reconstruction, Opt. Express 31, 19733-19745 (2023)

Ultra-intense laser characterization

Least-squares in Zernike-Taylor basis

$n_x \times x_y \times n_\omega \sim$ 1000x1000x100 numbers

$$Ax = y \xrightarrow{\text{Minimize}} \arg\min_x \{ ||Ax - y||^2 \}$$

Transform Ψ to (truncated) Zernike-Taylor basis

$$\arg\min_{\tilde{x}} \{ ||A\Psi\tilde{x} - y||^2 \}$$

Leading coefficients (<1000)

Much more robust reconstruction!

- A. Döpp et al. **Data-driven Science and Machine Learning Methods in Laser-Plasma Physics,** High Power Laser Science and Engineering **11** 55 (2023) | *arXiv:2212.00026* (2022)

Ultra-intense laser characterization

Compressed sensing

$n_x \times x_y \times n_\omega$ ~ 1000x1000x100 numbers

$$Ax = y \xrightarrow{\text{Minimize}} \underset{x}{\arg\min}\{\|Ax - y\|^2\}$$

Transform to some sparse basis (e.g. wavelet, PCA, etc.)

$$\underset{\tilde{x}}{\arg\min}\{\|A\Psi\tilde{x} - y\|^2 + \|\tilde{x}\|_1\}$$

Few coefficients as possible

- A. Döpp et al. **Data-driven Science and Machine Learning Methods in Laser-Plasma Physics,** High Power Laser Science and Engineering **11** 55 (2023) | *arXiv:2212.00026* (2022)

Ultra-intense laser characterization

Deep compressed sensing

$n_x \times x_y \times n_\omega \sim$ 1000x1000x100 numbers

$$Ax = y \xrightarrow{\text{Minimize}} \arg\min_x \{ \|Ax - y\|^2 \}$$

Transform to some sparse basis
(e.g. wavelet, PCA, etc.)

$$\arg\min_{\tilde{x}} \{ \|A\Psi\tilde{x} - y\|^2 + \mathcal{S}(y) \}$$

Learnt regularization
(Residual estimate)

- A. Döpp et al. **Data-driven Science and Machine Learning Methods in Laser-Plasma Physics,** High Power Laser Science and Engineering **11** 55 (2023) | *arXiv:2212.00026* (2022)

Ultra-intense laser characterization

Deep compressed sensing

$$Ax = y$$

$$\hat{x} = \arg\min_{\tilde{x}} \{ ||A\Psi\tilde{x} - y||^2 + \mathcal{S}(y) \}$$

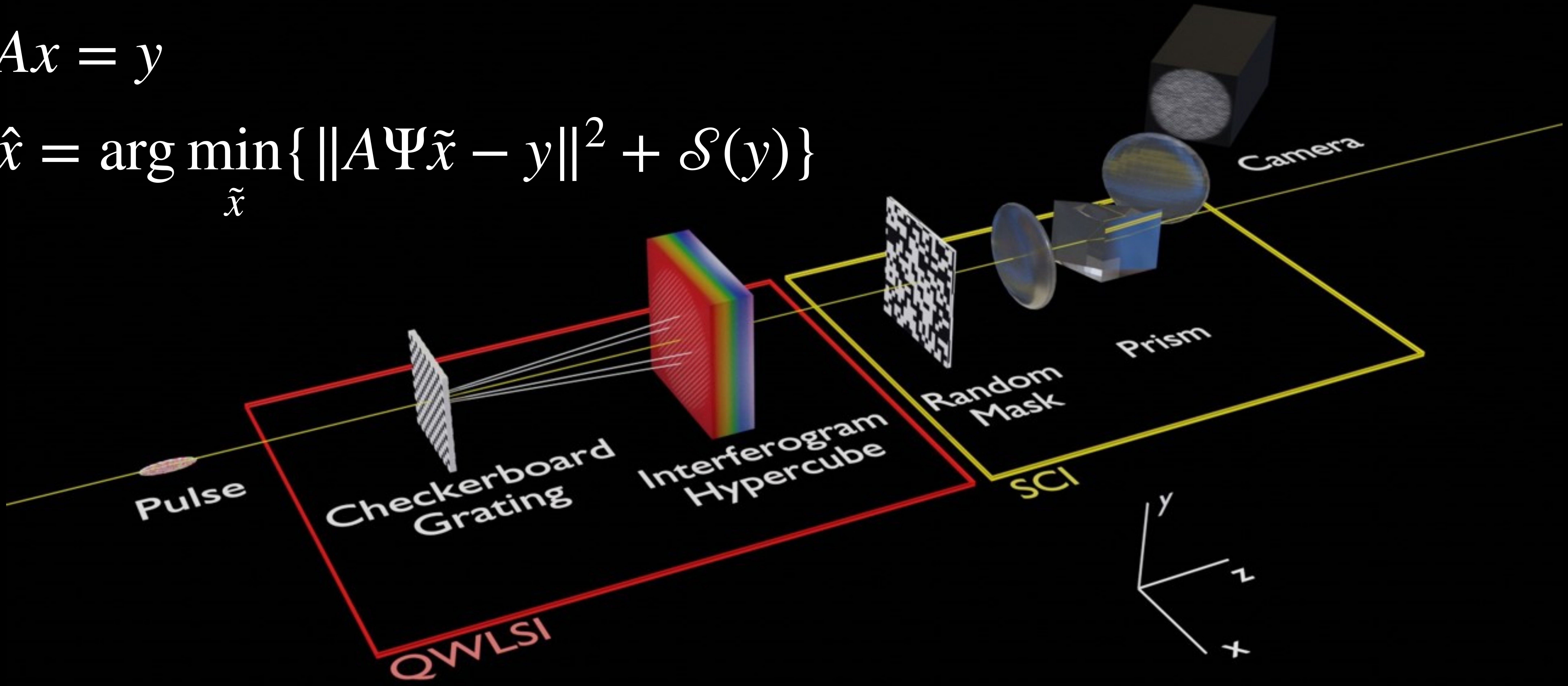

1. S. Howard et al. **Hyperspectral Compressive Wavefront Sensing**, High Power Laser Science and Engineering, 2023, 11(3):32

Bayesian optimization

Sequential model-based optimization

More on Bayesian optimization tomorrow in WG7!

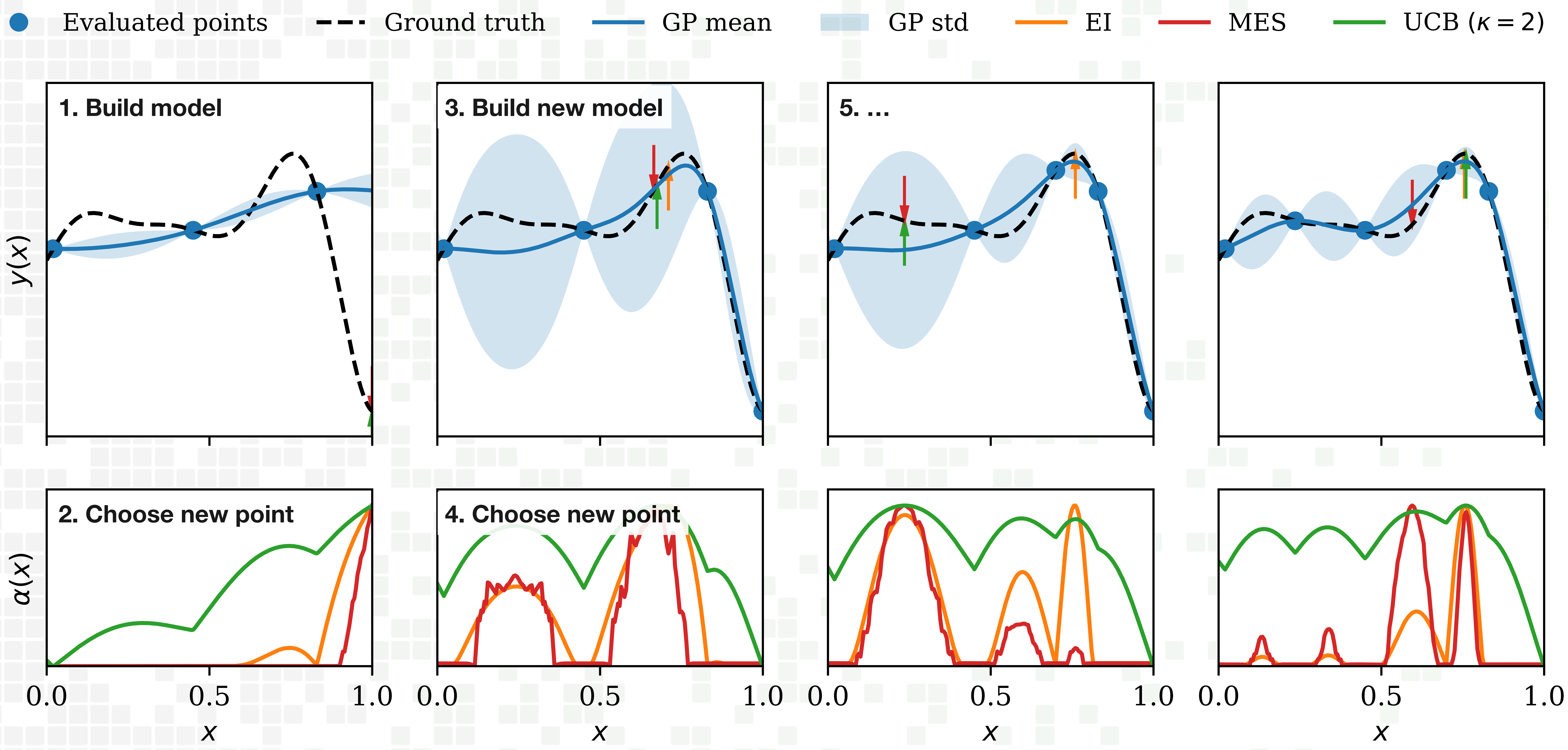

Multi-objective multi-fidelity optimization

Optimization of electron beam properties (FBPIC simulations)

- We want to optimize three electron beam parameters:
  - Charge Q (total charge, charge within FWHM, etc.)
  - Bandwidth (standard deviation σ_E, median absolute deviation E_{MAD}, etc.)
  - Distance to a target energy $|E_{target} - E|$ (using mean energy, median energy, peak energy, etc.)

- Choosing **different metrics or weights** for each objective **changes the outcome in an a priori unknown way**!
- Instead we want to make a survey and **learn the trade-offs** between all objectives (Pareto optimization)

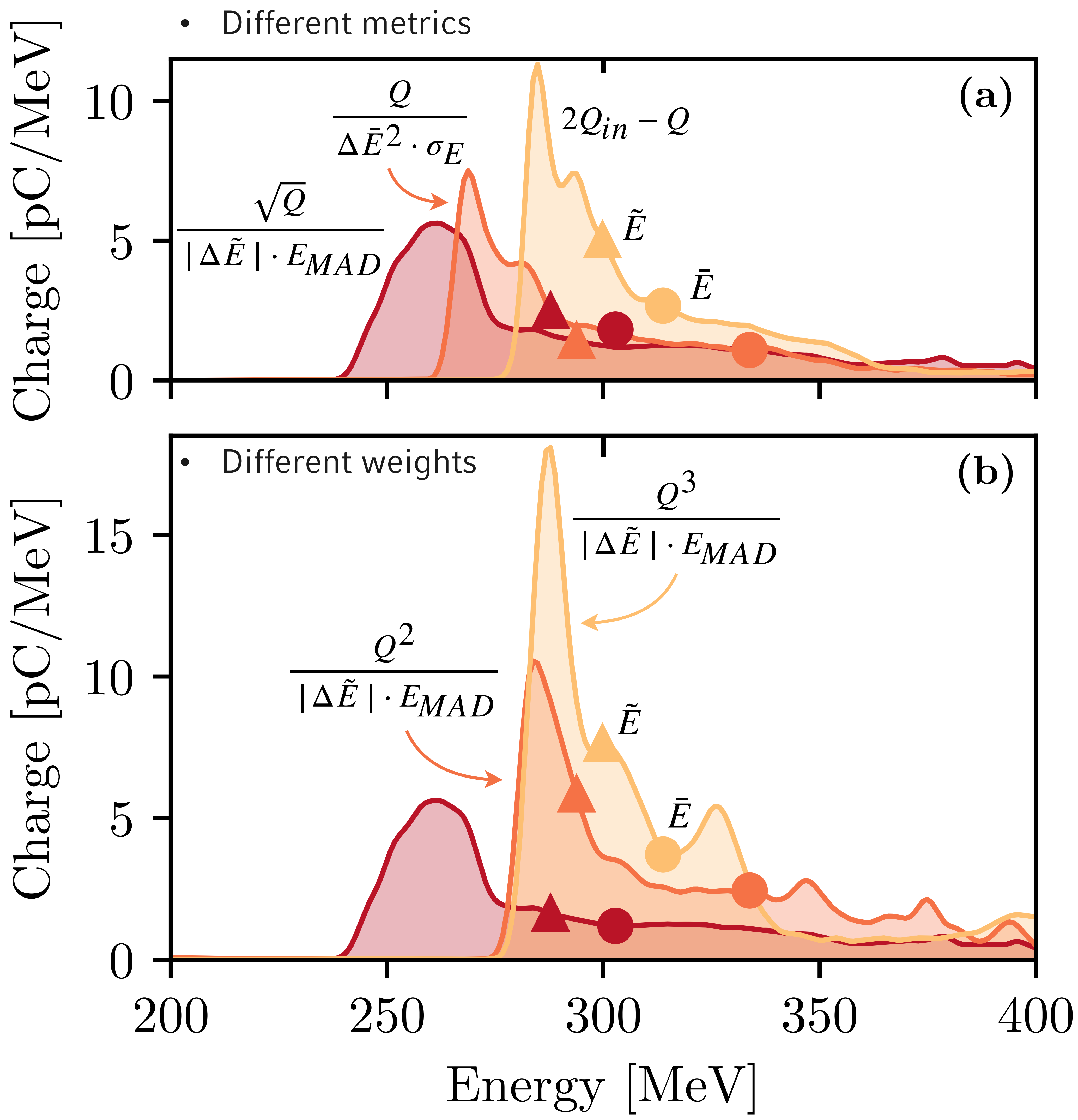

- Irshad, F., Karsch, S., & Döpp, A. **Multi-objective and multi-fidelity Bayesian optimization of laser-plasma acceleration**. *Phys. Rev. Research 5, 013063 (2023)*

Multi-objective multi-fidelity optimization

Optimization of electron beam properties (Experiment)

See Faran's talk tomorrow at 17:40 in WG7

8-D optimization:

- Jet focus & height,
- Blade focus & height,
- Dispersion (ϕ_2, ϕ_3, ϕ_4)
- Gas Pressure

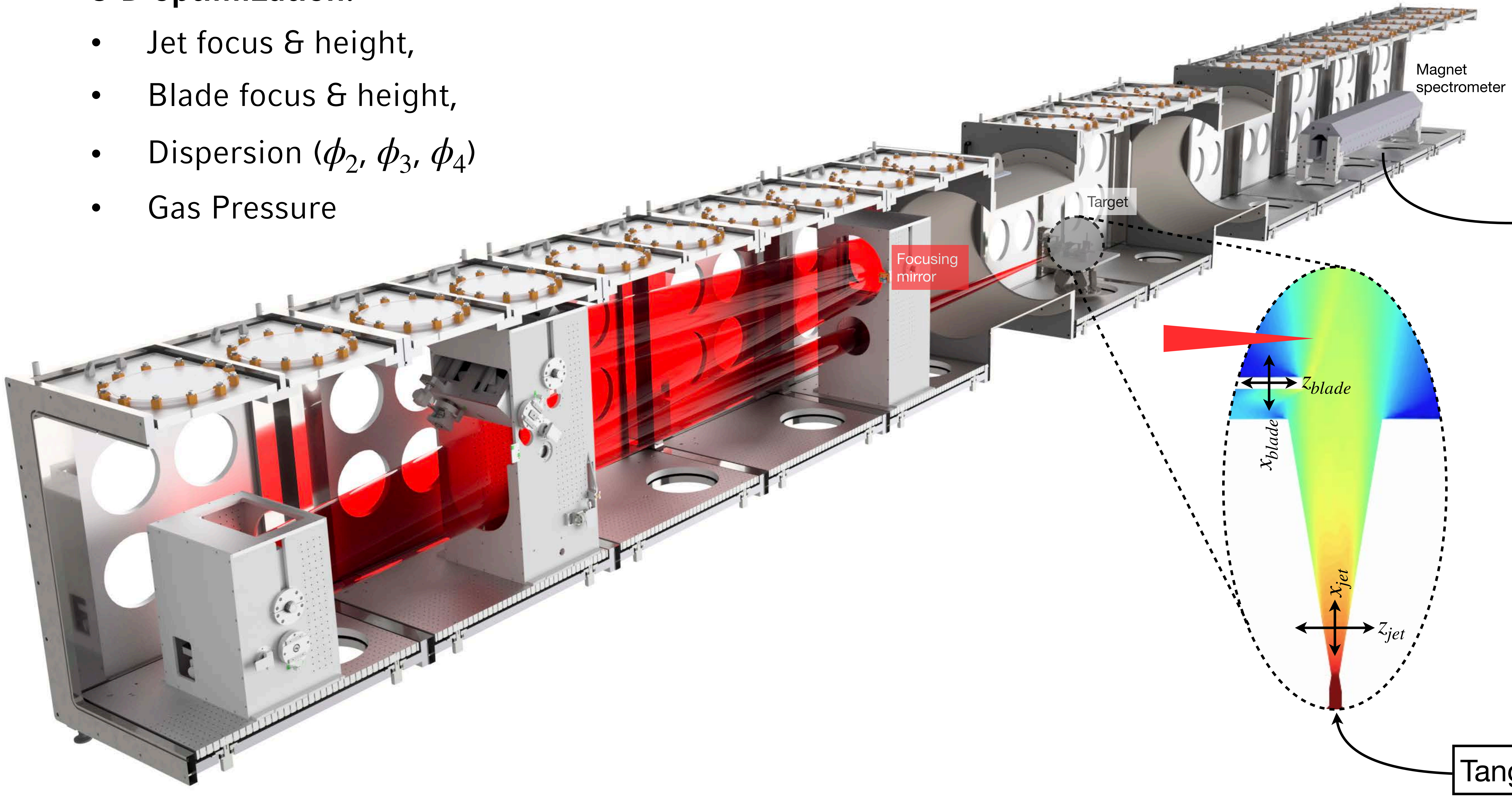

(Model chooses shot number dynamically)

Spectra at one position

Gaussian Mixture Model

↓

Extract objective values (Q, μ_E, σ_E, ...)

↓

Gaussian Process Model

↓

Expected Hypervolume Improvement

↓

Tango controls

- F. Irshad, et al. **Pareto Optimization of a Laser Wakefield Accelerator** *(under review)*

Multi-objective multi-fidelity optimization

Optimization of electron beam properties (Experiment)

- Once the Pareto-optimal solutions are identified, we can choose from them what kind of beam we want.
- We observe that many of the Pareto-optimal solutions yield the **same laser-to-beam efficiency**.
- Lower energy spread results in lower efficiency, i.e. is mostly a filtering effect

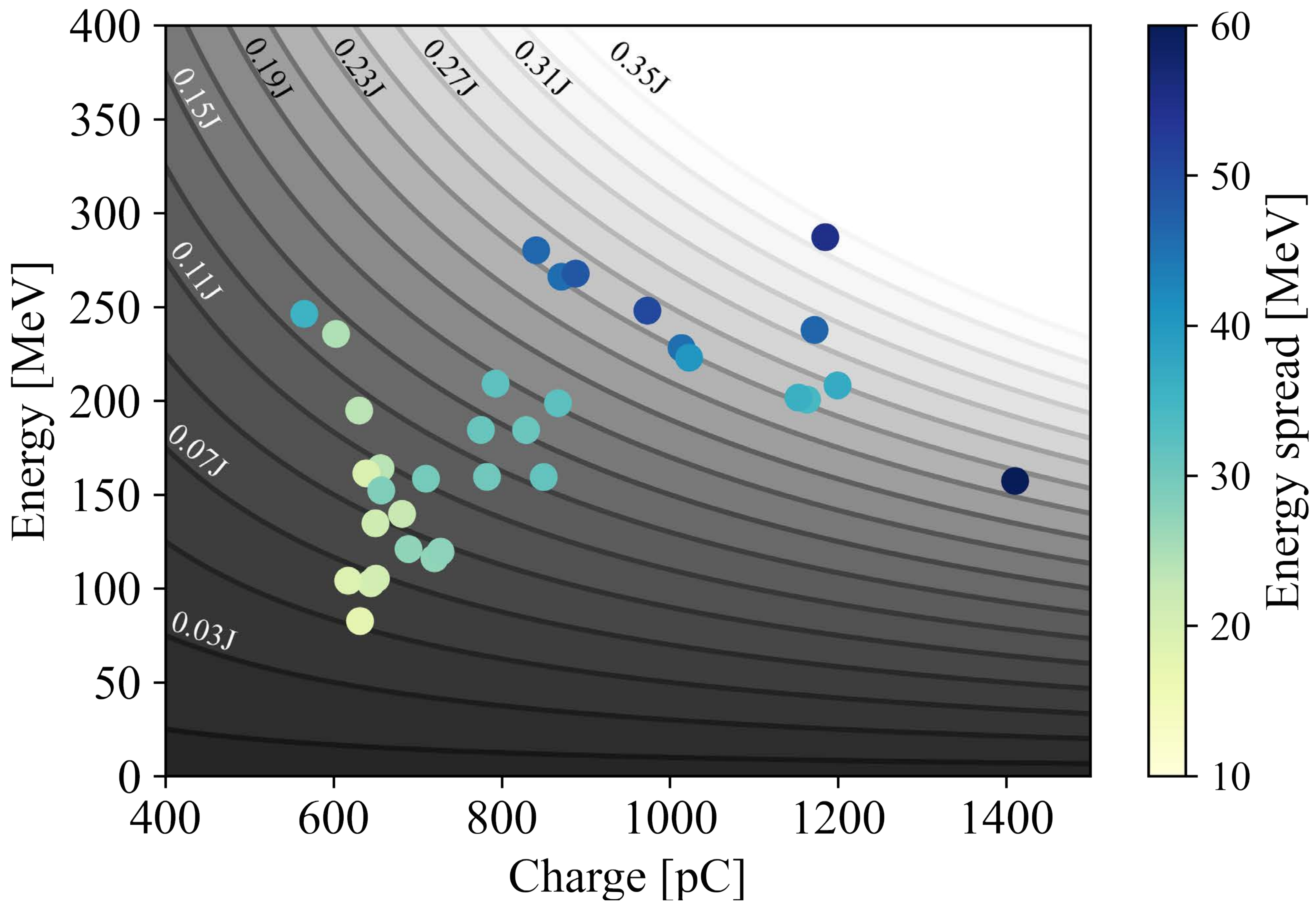

- F. Irshad, et al. **Pareto Optimization of a Laser Wakefield Accelerator** *(under review)*

Summary

Implemented a coherent control system based on TANGO controls in CALA

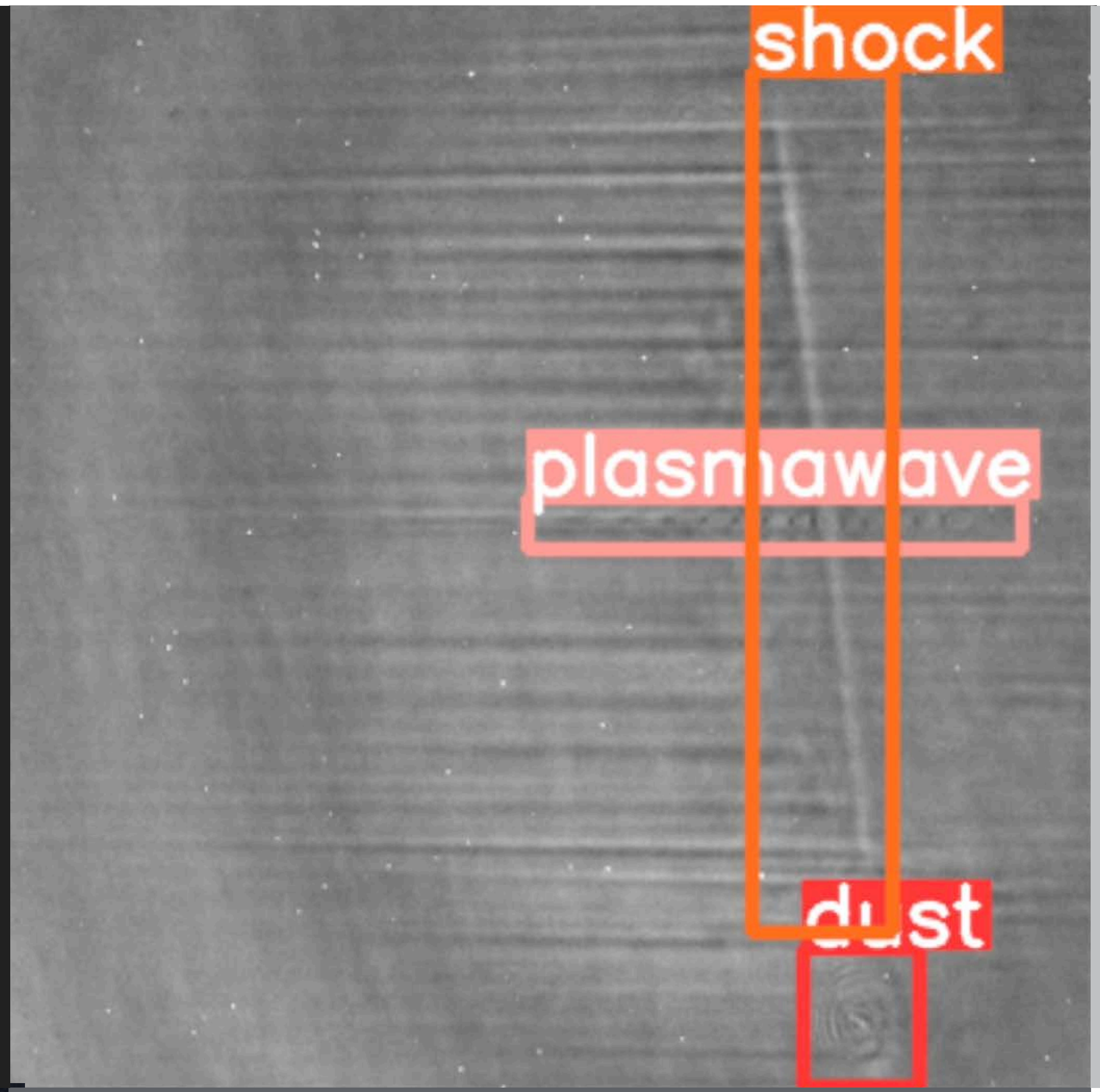

Demonstrated Few-Shot Spatio-Temporal Characterization in a Zernike-Taylor Basis

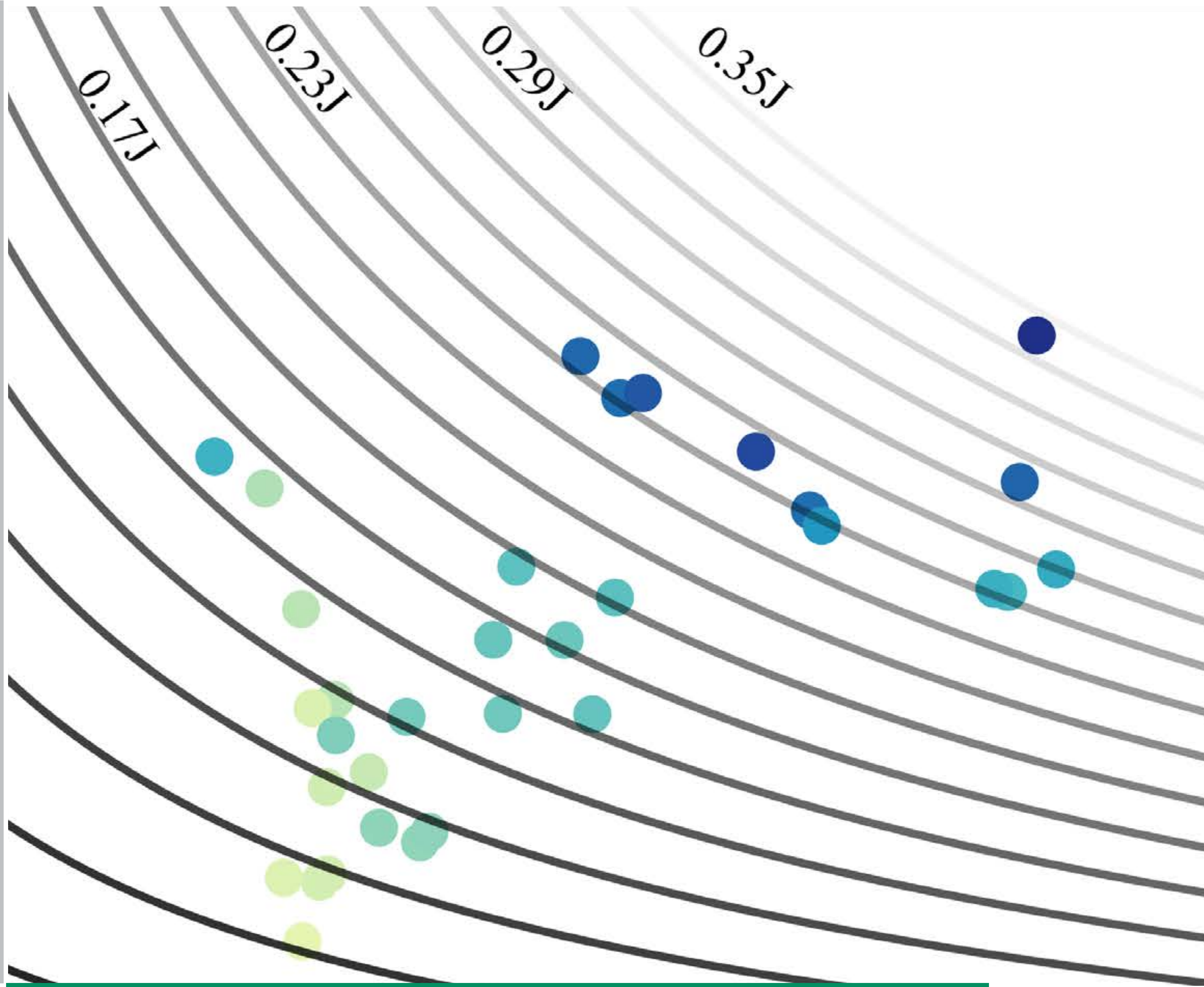

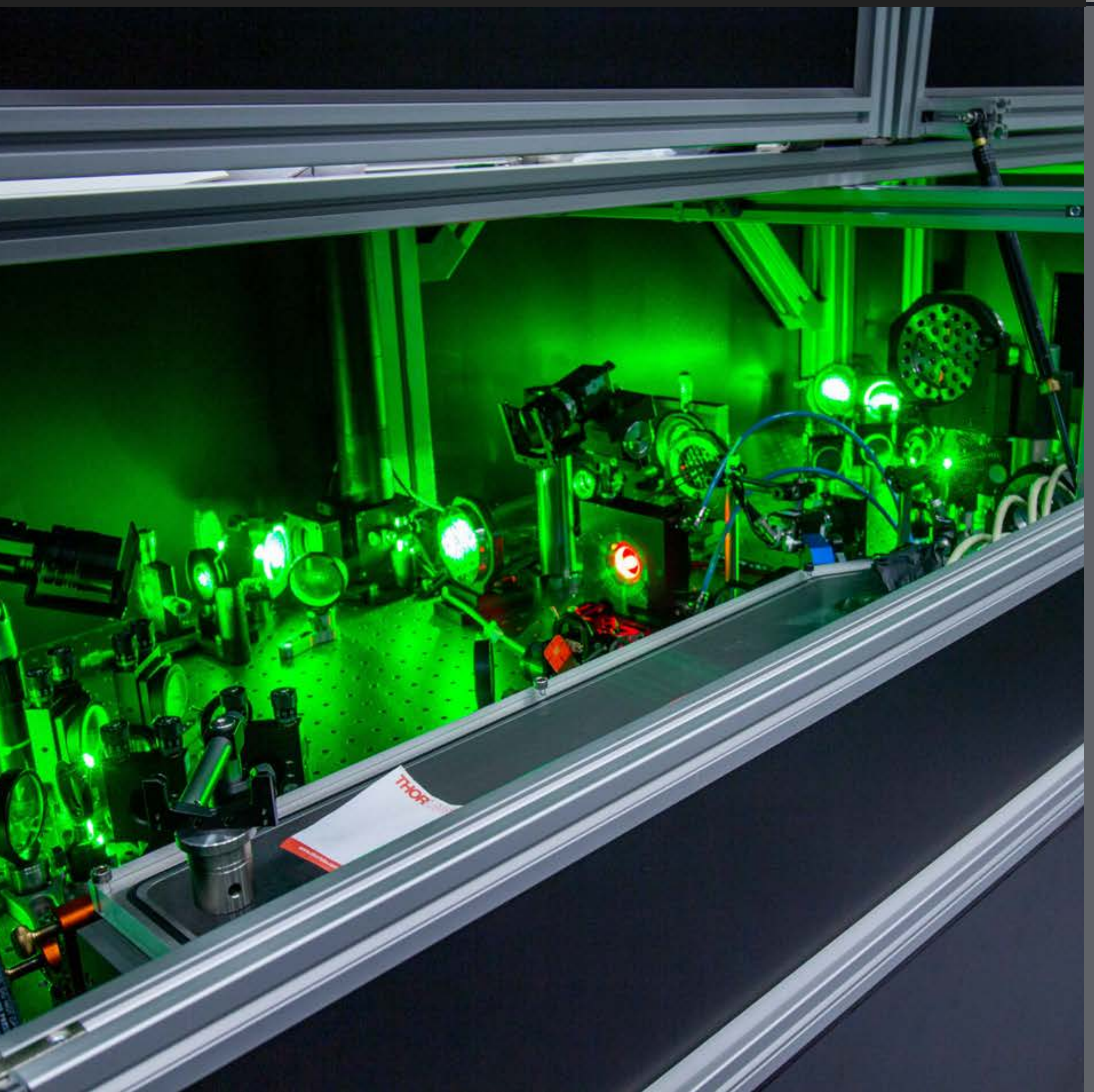

„Off-the-shelf“ ML:

Fine-tuned YOLO Object Detection to work with data from experiments

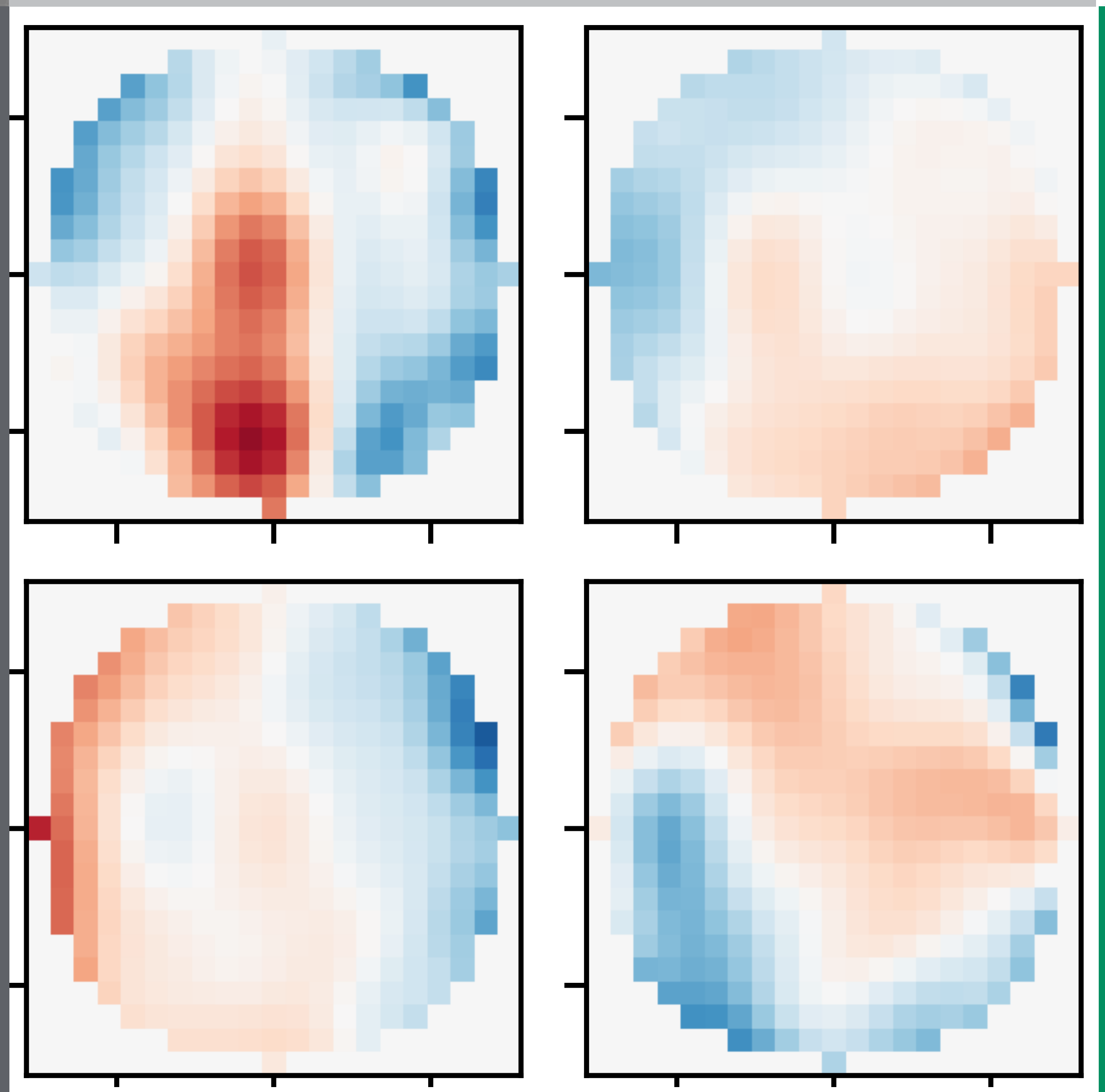

Demonstrated tuning of a laser-plasma accelerator with Bayesian optimization

LUDWIG-
MAXIMILIANS-
UNIVERSITÄT
MÜNCHEN

Thank you for your attention!

Dr. Andreas Döpp
Am Coulombwall 1 · 85748 Garching · Germany
a.doepp@lmu.de · www.pulse.physik.lmu.de